This Accepted Manuscript has not been copyedited and formatted. The final version may differ from this version.

eNeuro

Research Article: New Research | Integrative Systems

Distribution, Amplitude, Incidence, Co-occurrence, and Propagation of Human K-Complexes in Focal Transcortical Recordings

Localization and Characterization of K-Complexes

Rachel A. Mak-McCully[1], Burke Q. Rosen[2], Matthieu Rolland[2], Jean Régis[4,5,6], Fabrice Bartolomei[4,5,6], Marc Rey[4,5,6], Patrick Chauvel[4,5,6,*], Sydney S. Cash[7,*] and Eric Halgren[1,2,3,*]

[1]*Department of Neurosciences, University of California, San Diego, California, 92093, USA*

[2]*Department of Radiology, University of California, San Diego, California, 92093, USA*

[3]*Department of Psychiatry, University of California, San Diego, California, 92093, USA*

[4]*Aix-Marseille Université, Marseille 13385, France*

[5]*INSERM, Institut de Neurosciences des Systèmes UMR 1106, Marseille 13005, France*

[6]*APHM (Assistance Publique–Hôpitaux de Marseille), Timone Hospital, Marseille 13005, France*

[7]*Department of Neurology, Massachusetts General Hospital and Harvard Medical School, Harvard University, Boston, Massachusetts, 02114, USA*

DOI: 10.1523/ENEURO.0028-15.2015

Received: 2 April 2015

Revised: 9 July 2015

Accepted: 24 July 2015

Published: 2 September 2015

Author Contributions: RMM-M, PYC, SSC and EH Designed Research, RMM-M, BQR, SSC and EH Performed Research, BQR, MR1, JR, FB, PYC Contributed Unpublished Reagents/Analytic Tools, RMM-M, BQR, M. Rolland, JR, M. Rey, SSC and EH Analyzed Data, RMM-M and EH Wrote the Paper

Funding: NIH: R01 MH099645. National Science Foundation Graduate Research Fellowship; Chateaubriand Fellowship; Multidisciplinary University Research Initiative (MURI): ONR N00014-13-1-0672.

Conflict of Interest: Authors report no conflict of interest.

Co-senior authors

Correspondence should be addressed to: Rachel Mak-McCully, Multimodal Imaging Laboratory, UC San Diego, 9500 Gilman Drive, Mail Code 0841, La Jolla, CA 92093, (858) 534-8259, E-mail: rmakmccu@ucsd.edu

Cite as: eNeuro 2015; 10.1523/ENEURO.0028-15.2015

Alerts: Sign up at eneuro.org/alerts to receive customized email alerts when the fully formatted version of this article is published.

Accepted manuscripts are peer-reviewed but have not been through the copyediting, formatting, or proofreading process.

This is an open-access article distributed under the terms of the Creative Commons Attribution 4.0 International (http://creativecommons.org/licenses/by/4.0), which permits unrestricted use, distribution and reproduction in any medium provided that the original work is properly attributed.

Copyright © 2015 Society for Neuroscience

eNeuro Accepted Manuscript

eNeuro Accepted Manuscript

eNeuro

http://eneuro.msubmit.net

eN-NWR-0028-15R1

Distribution, amplitude, incidence, co-occurrence, and propagation of human K-Complexes in focal transcortical recordings

This is a confidential document and must not be discussed with others, forwarded in any form, or posted on websites without the express written consent of eNeuro.

eNeuro Accepted Manuscript

Manuscript Title: Distribution, amplitude, incidence, co-occurrence, and propagation of human K-Complexes in focal transcortical recordings

Abbreviated Title: Localization and characterization of K-complexes

Rachel A. Mak-McCully[1], Burke Q. Rosen[2], Matthieu Rolland[2], Jean Régis[4,5,6], Fabrice Bartolomei[4,5,6], Marc Rey[4,5,6], Patrick Chauvel[4,5,6^], Sydney S. Cash[7^], Eric Halgren[1,2,3^]

[1]Department of Neurosciences, [2]Department of Radiology, [3]Department of Psychiatry, University of California, San Diego, California, 92093, USA, [4]Aix-Marseille Université, 13385, Marseille, France, [5]INSERM, Institut de Neurosciences des Systèmes UMR 1106, 13005, Marseille, France, [6]APHM (Assistance Publique–Hôpitaux de Marseille), Timone Hospital, 13005, Marseille, France, [7]Department of Neurology, Massachusetts General Hospital and Harvard Medical School, Harvard University, Boston, Massachusetts, 02114, USA.

^ co-senior authors

Author Contributions: RMM, PC, SC and EH Designed Research, RMM, BQR, SC and EH Performed Research, BQR, MR1, JR, FB, PC Contributed Analytic Tools, RMM, BQR, MR1, JR, MR2, SC and EH Analyzed Data, RMM and EH Wrote the Paper

Correspondence should be addressed to:
Rachel Mak-McCully
Multimodal Imaging Laboratory
UC San Diego, 9500 Gilman Drive, Mail Code 0841

eNeuro Accepted Manuscript

La Jolla, CA 92093

(858) 534-8259

rmakmccu@ucsd.edu

Number of Figures: 13

Number of Tables: 3

Number of Multimedia: 0

Number of words for Abstract: 250

Number of words for Significance Statement: 119

Number of words for Introduction: 750

Number of words for Discussion: 2943

Acknowledgements:

The authors wish to dedicate this work to Frederic Sauvaget, an exceptional neurosurgeon, neuroscientist, and colleague. His passion for his work was truly inspirational.

In addition, the authors wish to thank neurosurgeons Romain Carron, Didier Scavarda, and Emad Eskandar for patient implantations. Special thanks to Catherine Liegeois-Chauvel for assistance in electrode localizations, facilitating research access, and scientific support.

Conflict of Interest

Authors report no conflict of interest.

Funding sources

eNeuro Accepted Manuscript

This material is based upon work supported by NIH grant number R01 MH099645, MURI: ONR N00014-13-1-0672, the National Science Foundation Graduate Research Fellowship, and the Chateaubriand Fellowship.

Full human subject recruitment statement:
Stereoencephalographic (SEEG) recordings were obtained in nine patients (eight women, one man; age: 41.4 ±4.9) suffering from pharmaco-resistant epilepsy to localize their seizure focus prior to possible resection at Massachusetts General Hospital or La Timone Hospital (Table 1).

Abstract

K-complexes are thought to play a key role in sleep homeostasis and memory consolidation; however, their generation and propagation remain unclear. The commonly held view from scalp EEG is that KCs are primarily generated in medial frontal cortex and propagate parietally, whereas an ECOG study suggested dorsolateral prefrontal generators and an absence of KCs in many areas. In order to resolve these differing views, we used unambiguously focal bipolar depth electrode recordings in patients with intractable epilepsy to investigate spatiotemporal relationships of human KCs. KCs were marked manually on each channel and local generation was confirmed with decreased gamma power. In most cases (76%), KCs occurred in a single location, and rarely (1%) in all locations. However, if automatically-detected KC-like phenomena were included, only 15% occurred in a single location and 27% in all recorded locations. Locally-generated KCs were found in all sampled areas, including cingulate, ventral temporal, and occipital cortices. Surprisingly, KCs were smallest and occurred least frequently in anterior prefrontal channels. When KCs occur on two channels, their peak order is consistent in

eNeuro Accepted Manuscript

only 13% of cases, usually from prefrontal to lateral temporal. Overall, the anterior-posterior separation of electrode-pairs explained only 2% of the variance in their latencies. KCs in stages two and three had similar characteristics. These results open a novel view where KCs overall are universal cortical phenomena, but each KC may variably involve small or large cortical regions, and spread in variable directions, allowing flexible and heterogeneous contributions to sleep homeostasis and memory consolidation.

Significance Statement

This is the first examination of the location of KCs and their temporal relationship across the cortex using such focal measures of brain activity. KCs, along with sleep spindles and slow oscillations, are thought to play important roles in the restorative and memory consolidation processes of non-REM sleep. KCs are unique from these other markers because they indicate isolated periods of cortical silence. We describe here that KCs occur in parts of the brain previously thought not to generate KCs. We show they may co-occur over small or large parts of the cortex, but do not propagate in a systematic way. This variability could reflect and support consolidation processes devoted to memories involving the corresponding cortical areas and sequences.

Introduction

K-complexes (KCs) are isolated downstates occurring both spontaneously and in response to sensory stimuli during NREM sleep (Colrain, 2005; Cash et al., 2009). Here we examine the spatial distribution and temporal dynamics of KCs across the cortex using bipolar SEEG (stereoencephalographic) recordings to address basic questions that are unanswered or

eNeuro Accepted Manuscript

93 ambiguous in the KC literature: which cortical regions generate KCs? How variable is KC
94 amplitude? How variable is KC occurrence rate? How often do KCs co-occur across the cortex?
95 Do KCs propagate sequentially from one cortical location to another?
96 Answers to some of these questions have varied due to recording technique. Scalp EEG
97 examination of the KC indicates that KCs are largest in amplitude and most frequent over
98 midline frontal sites (Colrain, 2005; Halasz, 2005). Cortical surface ECOG recordings and
99 average reference SEEG recordings have led to the conclusion that many cortical areas crucial
100 for memory do not generate KCs (Wennberg, 2010). Scalp EEG and ECOG recordings,
101 however, are difficult to interpret due to potential overlap and cancellation from multiple
102 distributed generators. Additionally, average references may detect signals that are not locally
103 generated.
104 Bipolar SEEG recordings eliminate the ambiguity of scalp EEG, ECOG, and average reference
105 SEEG. In both scalp EEG and ECOG, individual electrodes record activity from local and
106 distant generators, which are difficult to disentangle; scalp EEG is further smeared by the skull.
107 In bipolar SEEG recordings, nearby contacts along an electrode are subtracted from one another.
108 Adjacent contacts chosen for analysis can have one contact just above the grey matter in the
109 CSF, and one just below the grey matter in the white matter. This subtraction provides a focal
110 recording of brain activity unavailable with scalp EEG or ECOG. Even the use of an average
111 reference in SEEG may mask or augment a local signal, which is not the case when SEEG is
112 analyzed using bipolar subtraction. The ambiguity inherent in scalp EEG, ECOG, and referential
113 SEEG may confound interpretations of both where KCs are generated and how they co-occur or
114 spread across the cortex.

eNeuro Accepted Manuscript

115 Another source of ambiguity in previous studies is the grouping together of KCs and slow
116 oscillations (SOs), which occur as a series of up and downstates in NREM stage 3. SOs and KCs
117 share a frequency of ~1Hz and the KC is identical to the downstate of the SO (Cash et al., 2009).
118 The commonly-used automated SO detection methods identify all large low frequency
119 deflections, including KCs. Scalp EEG recordings have led to the interpretation that SOs
120 propagate across the cortex in an anterior to posterior direction, with a delay of ~200ms
121 (Massimini et al., 2004; Murphy et al., 2009). Since these studies included KCs as well as SOs in
122 their analyses, these studies provide insight into the propagation of KCs as well. A major
123 distinction between SOs and KCs remains that the KC is an isolated event: it is neither part of an
124 ongoing oscillation nor preceded by an upstate. It is, therefore, possible to pinpoint the start of a
125 KC in the cortex. In contrast, because the SO is an oscillation, it can be difficult to determine
126 which waves correspond to each other across different cortical areas, resulting in ambiguous
127 order and dependence.
128 By rigorously quantifying the spatial distribution and temporal dynamics of KCs across the
129 cortex, we focused on three questions. First, are KCs a fundamental neocortical state that are
130 locally generated in all neocortical areas with similar amplitudes and rates of occurrence?
131 Particular attention was paid to the cingulate, ventral temporal, and occipital cortices where
132 Wennberg (2010) failed to find KC generators using intracranial recordings. Similarly, special
133 attention was paid to lateral cortex, in general, where other studies using high-density EEG
134 failed to find generators of evoked KCs or isolated SOs, i.e. KCs (Murphy et al., 2009; Riedner
135 et al., 2011). Second, do KCs co-occur in multiple lobes and both hemispheres, or do they occur
136 in a more isolated fashion? Third, do KCs systematically propagate from anterior to posterior
137 locations, and in particular from prefrontal to parietal?

eNeuro Accepted Manuscript

The three NREM sleep markers —sleep spindles, SOs, and KCs—have all been implicated in the restorative and memory processes which occur during sleep (Diekelmann and Born, 2010; Tononi and Cirelli, 2014). By understanding where the KC occurs in the brain, how the KC occurs temporally across the cortex, and whether it is an event that may manifest heterogeneously each time it occurs, we can understand how each generating structure's role and their orchestration leads to sleep homeostasis and memory consolidation.

Materials & Methods

Stereoencephalographic (SEEG) recordings were obtained in nine patients (eight women, one man; age: 41.4 ±4.9) suffering from pharmaco-resistant epilepsy to localize their seizure focus prior to possible resection at Massachusetts General Hospital or La Timone Hospital (Table 1). Anatomical nomenclature follows Destrieux et al. (2010). At Massachusetts General Hospital, electrodes were localized with respect to anatomical structures using CT with the electrodes in place, and intraoperative photographs (Dykstra et al., 2012). Depth electrodes (SEEG) either had 8 contacts with 5mm center-to-center spacing or 6 contacts with 8mm center-to-center spacing. Each contact was 2.4mm long with a diameter of 1.28mm. The electrodes usually passed approximately perpendicular to the midsagittal plane. At La Timone Hospital, electrodes were localized using the fusion of CT with implanted electrodes and MRI. In one case, surgical planning and pre-operative MRI was used to localize the electrodes. SEEG electrodes had 10 or 15 contacts with 3.5mm center-to-center spacing; in some cases the 15 contact electrodes contained three sets of five contacts, with 3.5mm center-to-center spacing within set and 7 or 11mm between each set of five contacts. Contacts were 2mm long with .8mm diameter. Electrodes were both perpendicular and oblique. Prior to surgery, fully informed consent was

eNeuro Accepted Manuscript

obtained under the auspices of local institutional review boards. The signals were sampled at 256, 500, 512, or 1024Hz.

Adjacent contacts along each SEEG electrode were subtracted to create bipolar contacts. The bipolar derivation was obtained by subtracting the more lateral lead from the more medial adjacent lead. In the case where the electrode is passing through the most superficial cortex, the lateral lead is over the pia and the medial is in the underlying white matter. Since the KC is surface-negative (Cash et al., 2009), a medial-minus-lateral derivation would in this case result in a positive peak. In contrast, at the midline locations (for example, the crown of the cingulate gyrus), the medial lead is above the pia and the lateral is in the underlying white matter, and consequently KCs are negative in the medial-minus-lateral derivation. Intermediate bipolar pairs could be either polarity depending upon the exact relationship of the contacts to local cortical folding.

Contacts to include for analysis were chosen by examining both physiological and anatomical criteria. Physiologically, referential recordings from a given depth electrode were examined for successive contacts which recorded polarity-inverted spontaneous activity. In such cases, anatomically, one contact of the bipolar pair would typically lay in the CSF above the cortical grey matter while the other lay just below it in the white matter. In the case of overlapping bipolar contacts (i.e. two pairs sharing a contact) only one bipolar pair was included for analysis. A total of 55 bipolar contacts were analyzed. This bipolar method is free of volume conduction and reference lead issues, obtaining unambiguously focal cortical recordings. Furthermore, to be included for analysis, contacts needed to be distant from the epileptogenic focus, free of epileptiform activity (spikes or pathological slowing), and exhibit K-complexes (KCs).

eNeuro Accepted Manuscript

Usable scalp EEG channels were recorded in the four subjects from Massachusetts General Hospital, but not the five subjects from La Timone Hospital. When present, the scalp recordings lacked the full montage used for formal polysomnography (Silber et al., 2007). Periods when patients were behaviorally noted to be sleeping were selected for analysis. As this study sought to characterize KCs as measured locally, rather than defined by scalp EEG, initial selection of KCs was blind to sleep staging. As a secondary analysis, sleep staging based on scalp EEG—as well as EMG and EOG, when available--for subjects recorded at Massachusetts General Hospital, or based on the SEEG for subjects recorded at La Timone Hospital, was performed for all subjects by a qualified rater (Marc Rey).

KCs were manually marked independently on each bipolar SEEG contact for each subject. Each night was considered independent and studied separately. Selected KCs were isolated (i.e. not part of a preceding oscillation) and exhibited a multiphasic morphology, with a significant drop peaking ~500ms from the beginning of the waveform, often followed by a rebound peaking at ~900ms (Colrain, 2005). Each channel was then band-passed from 0.1 to 5Hz in order to select the peak of the manually-marked KC.

To confirm that selected KCs, regardless of their polarity, were downstates, we tested for a drop in high gamma power (HGP) at the time of the KC in all channels for each subject. If a subject had multiple nights, only one sample night was used to test HGP drop in all channels. KCs were therefore not validated individually for a drop in HGP, but validated over all KCs in each channel, for one night per subject. HGP was calculated from 60 to 120Hz, or 70 to 120Hz, depending on whether the line noise was at 50Hz or 60Hz, respectively. Visually, a drop in HGP up to 120Hz was determined by a time frequency analysis using default wavelets in EEGLAB (Delorme and Makeig, 2004): with the most negative peak of the KC at time zero, -1.5 to -0.5

eNeuro Accepted Manuscript

206 seconds was used as a comparison baseline for a t-test at a $p<0.01$, uncorrected threshold. The
207 drop in HGP seen at the time of the KC was further verified using a Hilbert transform applied to
208 each KC. The analytic amplitude of the Hilbert transform was calculated after applying a band
209 pass filter for the appropriate HGP range (either 60 to 120Hz or 70 to 120Hz) and averaged over
210 all KCs for each channel. Compared to a baseline period from -1.5 to -1 seconds prior to the
211 most negative peak of the KC at time zero, periods of significant ($p<0.01$, t-test, FDR corrected)
212 drop in HGP were required for KC confirmation. These analyses were accomplished with custom
213 Matlab (MATLAB, 2009) routines with dependencies including the FieldTrip (Oostenveld et al.,
214 2011) toolbox.
215 In order to compare our bipolar derivations to the common average reference recordings used in
216 a previous study (Wennberg, 2010), referential recordings were reconstructed for the individual
217 leads used in a typical transcortical bipolar pair, and in nearby leads on the same probe but in the
218 white matter. HGP was calculated as above (see Figure 3 for details).
219 KC detections were grouped across channels to classify the number of unique KC events for
220 each night for each subject using R (R Development Core Team, 2004). Starting with the first
221 KC peak, additional channels were classified as participating in the same KC if their peak time
222 was 200ms or less from this first peak latency. The next KC peak after the 200ms window was
223 the beginning of the second KC event. Grouping of KC events continued until the last KC peak
224 was classified. As a control, KCs were also regrouped using a 200ms crawling window: after
225 each KC peak detection, the detection window was shifted 200ms to the right. The detection
226 window continued shifting to the right until no more peaks were detected. These regroupings
227 were not used for any of the analyses described below.

eNeuro Accepted Manuscript

Although the 200ms window procedure would allow KCs occurring in at least two channels to have a maximum peak difference up to 200ms, the actual maximum difference was observed to be much less. This latency difference was quantified by calculating the delay between the first channel peak and the last channel peak for each KC event. The mean and standard deviation over all KCs for each night was then calculated.

To study how KC amplitude and KC occurrence rate may vary across the cortex, bipolar channels were grouped by anatomical locations into 10 groups (see Figure 1). To test KC amplitude, a linear mixed effects model (Pinheiro et al., 2015) was performed. Location was used as a fixed effect. Placement of electrodes for each patient was chosen to localize the patient's epilepsy, but electrodes included in this analysis were not shown to be part of each patient's seizure focus. Therefore, patient and location were considered independent. Inter-patient variability was adjusted for by using patient as a random effect. Channel variability due to electrode placement with respect to the surrounding cortex, as well as variable contact spacing, was taken into account by using channel as a random nested effect.

To test KC occurrence rate, a linear mixed effects model of the inter-KC interval was performed with location as a fixed effect and patient as a random effect. In both the amplitude and occurrence rate models, the orbitofrontal cortex group served as the reference. For the residuals of the model to be normally distributed, a log transform was applied to the amplitudes and a Box-Cox Transform (Box and Cox, 1964) was applied to the inter-KC intervals. Normality of the residuals was checked visually. All models were developed using the LME procedure implemented in the nlme package (Pinheiro et al., 2015) of R. Due to the limitations of this package, confidence intervals for all predicted values derived from the linear mixed effects models could not be provided. In order to quantify the difference in either amplitude or

eNeuro Accepted Manuscript

occurrence rate between a tested location and the orbitofrontal reference, population level predictions were computed for each location. An inverse Box-Cox transformation was then applied to these estimates to obtain values in either μV or ms in order to compute a relative percentage to the reference level.

To test if KCs co-occur in multiple channels, we compared the number of KC events observed in exactly one channel, versus more than one channel, to what those numbers would be by chance. Fisher's exact test was performed in R to determine if they significantly differed at alpha=0.05. The number of KCs that would be expected in one channel or multiple channels by chance was estimated by randomizing the latencies between two consecutive KCs within each channel. This provided a new list of KC peaks for each channel. This randomization was performed 1000 times. These randomized latency differences were converted into latencies by adding in the latency of the first detected KC for each channel. Additionally, the latency of the first detected KC was added back to keep the number of latencies consistent. The KCs were then grouped for each of these 1000s simulations in the same manner as for the actual data (i.e., within 200ms time windows) to create the distribution of expected single and multi-channel KC events under the null hypothesis.

Using the same method for subjects with more than two channels, we tested co-occurrence for KCs observed in three or more channels, four or more channels, and five or more channels. Five or more KCs had to be observed for the category to be tested. Bonferroni correction for multiple comparisons was applied to all test results.

To test if KCs occur in a sequential order across the cortex, a multinomial test was performed in R for KC events observed in two, three, four, or five channels. The channel sequence of each KC event was determined by ordering channels by their KC peak latency. For a given set of

eNeuro Accepted Manuscript

channels, the multinomial test compares the frequencies of observed sequences to all possible sequences containing the same channels. Bonferroni correction was applied separately to each category of channels over all subjects.

Because each KC was verified visually, and for each channel, KCs were in all cases validated by decreased high gamma power, one may be confident in the locations where they were found to be locally generated and other quantified characteristics. However, using such strict criteria could lead to an underestimation of the extent of cortical involvement in a given KC event. This possibility was avoided by using an automatic procedure to look for KC-like activity in the channels where KCs were not manually marked, at times when a KC was manually marked in at least one channel. Each channel was band-passed with a zero phase-shift filter from 0.2 to 5Hz before detection of KC-like activity. For each channel, a KC template was created by averaging over the manual KC detections from -350 to +650ms around the peak. A sliding inner product was then performed between this template and a 1.2 second window when a manual KC occurred in at least one channel. To prevent edge effects, this window was set from -450 to +750ms around the manually marked KC peak at time zero; if more than one channel was manually marked, then the average of the first and last peak latency was used as time zero. The maximum value of the sliding inner product within the 200ms window where the template and test data overlap was compared to a predetermined threshold value. If this value was greater, the channel was considered to contain KC-like activity. However, if the time when the sliding inner product was greatest was at the edge of the 200ms window (and the amplitude continued to get larger beyond that window), then the activity was not counted as KC-like.

The threshold value for KC-like activity was determined for each channel by calculating the sliding inner product between the KC template and randomly-chosen epochs of data that did not

eNeuro Accepted Manuscript

297 contain KCs or slow oscillations in any channel. The number of such epochs chosen was 110%
298 the number of KC events for each night. As above, the maximum value of the 200ms window
299 where the template and each epoch overlapped was stored in a vector. The threshold was the
300 99^{th} percentile of that vector. Thus, the KC-like activity chosen by the template can be
301 considered to be more similar than random activity to the template constructed from the
302 manually chosen KCs at $p<.01$. For two nights in two different subjects, it was not possible to
303 obtain 110% the number of KC events. In these cases, approximately 350 periods for each
304 channel were used.
305 To quantify the characteristic differences between manual and template-detected KCs, the KC
306 peak amplitudes, and the signal variance from -1.4 to -0.4 seconds prior to the KC peak, were
307 calculated for each channel for the null times, manual KCs, and template-detected KCs. Z-
308 scores for the peak amplitude and variance on each channel for the manual and template-detected
309 KCs were calculated with respect to the null values. A paired t-test was calculated between the
310 z-scored manual KC amplitudes averaged over all channels and the z-scored template-detected
311 KC amplitudes averaged over all channels. Another paired t-test was calculated comparing pre-
312 KC period variance between average z-scored manual and template-detected KCs.
313 A new list of KC events, including KC-like activity in addition to the manually marked KCs was
314 computed. To test whether there is a consistent temporal relationship between manually-
315 detected and template-detected KCs, the difference between the average peak latency of all
316 manual KCs and the average of all template KCs was calculated for each KC event for a
317 representative night over all subjects.
318 The number of channels participating in KCs and the regional distribution of KCs was compared
319 between the manual-only KCs and the manual plus template-detected KCs. For one

eNeuro Accepted Manuscript

representative night for each subject, the number of KCs occurring on each channel was normalized to the largest number of KCs occurring on a channel. This normalization was performed separately for the manual only detections and the manual plus detections surviving the 99th percentile threshold. A multinomial test was repeated for these KCs to test if the inclusion of KC-like activity revealed any meaningful sequential order of two channels across the cortex. Bonferroni correction was applied to all tests.

To further test for a significant relationship between KC latency and anterior to posterior distance in the cortex, all pairs of anterior and posterior channels were chosen for each subject. Pairs were in all cases from different electrodes and could maximally have one contact gap in the medial-lateral direction. These three dimensional electrode coordinates were projected onto the sagittal plane. The distance between these coordinates for each channel pair was plotted versus the average KC latency difference between each pair. Additionally, the channel distance was plotted for each individual KC latency difference. Significant distance versus delay relationships were analyzed in a linear mixed effects model (Pinheiro et al., 2015), where the patient was introduced as a random effect to account for inter-individual variability. Marginal r squares were calculated as presented in (Nakagawa and Schielzeth, 2013).

Results

Cortical areas generating KCs

KCs were analyzed from nine patients undergoing observation for intractable epilepsy. A total of 55 bipolar SEEG contacts were included for analysis. Contacts sampled all lobes but showed the greatest concentration in subcallosal, prefrontal (anterior and posterior), and temporo-parieto-

eNeuro Accepted Manuscript

342 occipital junction regions (Figure 1A). Bipolar contact pairs spanned the grey matter, with one
343 contact in the white matter and the other in the CSF, providing a very focal measure (Figure 1B).
344 KCs were manually marked, independently on each bipolar channel. A total of 13,821 KCs were
345 manually marked over all channels for all subjects. For each channel, KCs were verified as
346 downstates by a significant drop in high gamma power at the time of the KC (Figure 2). Locally-
347 generated KCs were demonstrated in all sampled regions, including subcallosal, orbital,
348 cingulate (anterior and posterior), frontal (superior, middle and inferior, pars opercularis,
349 triangularis and orbitalis), supramarginal, angular, annectant, temporal (inferior and middle) gyri,
350 the insula and frontal operculum, and the central and anterior occipital sulci (Figure 2).
351 In addition to the 55 bipolar SEEG contacts included for further analysis, KCs were also
352 identified in four bipolar SEEG contacts where it has previously been reported that KCs are not
353 found (Wennberg, 2010). These sites were in anteroventral medial temporal (possibly
354 entorhinal), posteroventral medial temporal, and lateral ventral temporal areas. These four sites
355 were not included in further analyses because they either occurred in potentially non-isocortex
356 (entorhinal cortex) or were in locations implicated in the patient's epilepsy; therefore, further
357 verification is needed for these sites. As with the other pairs, these sites recorded locally
358 generated KCs, as verified by a significant drop in high gamma power (Figure 2, sites marked by
359 red squares).
360
361 **KCs measured in bipolar versus common average reference montage**
362 Previously, KC generation was examined using SEEG, with each individual electrode contact
363 referenced to a common average of scalp electrodes (Wennberg, 2010). To compare this method
364 to the method of transcortical bipolar subtraction used in the analyses presented here, KCs were

eNeuro Accepted Manuscript

examined in two adjacent white matter contacts, as well as two adjacent contacts spanning the grey matter, in both the common average reference and bipolar montage (Figure 3). All four contacts were located on the same electrode.

Using the KCs identified on the bipolar channel spanning the grey matter, the two white matter contacts referenced to the common scalp average show clear KCs (Figure 3A, red waveforms). However, when the two white matter channels are viewed in a bipolar montage (blue waveform), the signal is flat. This finding implies that the common average reference signal in this case is due to volume conduction rather than local generation. This interpretation is consistent with the absence of a drop in high gamma power in any bipolar or referential recording from the white matter contacts.

Conversely, the transcortical bipolar contact along the same electrode used in this study spans the grey matter, with one contact on the white matter side of a cortical patch, and the other on the CSF side. In this case, both channels referenced to the common scalp average show KCs (Figure 3B, red waveforms), but so does the bipolar subtraction between these two channels (blue waveform). Additionally, in all three cases, there is a drop in high gamma power to verify that what is being recorded is a downstate. Common average reference SEEG can, therefore, accurately record KCs, but it also risks recording activity that is not locally present, which is not the case for bipolar SEEG.

KC amplitude and occurrence rate varies across cortical locations.

In Figure 4A, average KC amplitudes for each channel are color-coded by subject. The mean amplitudes in μV for subjects 1 through 9 were: 416, 329, 209, 489, 385, 513, 420, 624, and 230. The largest amplitude KCs were recorded in posterior prefrontal and anterior

eNeuro Accepted Manuscript

cingulate/subcallosal areas, whereas small KCs were recorded in anterior prefrontal and orbital areas, and moderate amplitude KCs were recorded in ventrolateral temporal areas (Figures 2 & 4A). Large KCs were also recorded in supramarginal, posterior cingulate, and anterior occipital areas, although sampling was limited. It should be appreciated that low amplitudes could reflect individual variation between patients, in exact electrode placement with respect to the cortex, or in variable spacing between contacts, rather than a characteristic of a particular cortical area.

In order to account for these patient and channel variabilities, a linear mixed effects model of the amplitudes was performed with location as a fixed effect, patient as a random effect, and channel as a random nested effect. Bipolar channels were grouped into 10 locations by anatomic location, as pictured in Figure 1. The results of the model revealed that there were no significant amplitude differences between areas, although the anterior prefrontal cortex was close to being significantly smaller ($p=0.089$), despite the common observation that the largest scalp KCs are recorded above this area. These issues are further examined below.

In Figure 5A, the occurrence rate in each bipolar pair was normalized to the pair with the highest frequency in that subject, resulting in less striking differences between cortical locations. As a measure of occurrence rate, the inter-KC intervals were calculated for each channel. A linear mixed effects model of these intervals was calculated with location as a fixed effect and patient as a random effect to test for areas with significantly different occurrence rates. Compared to the orbitofrontal reference, KCs occurred 15% more often in the anterior cingulate ($p=0.0051$), 48% more in posterior cingulate ($p<0.00001$), 11% more in posterior prefrontal ($p=0.024$), and 14% more in ventrolateral temporal regions ($p=0.022$); these groups are highlighted in pink in Figure 5A. Again, contrary to inferences from scalp EEG findings, KCs occurred 30% less often in the anterior prefrontal cortex ($p=0.0001$) compared to the orbitofrontal location. KCs also occurred

eNeuro Accepted Manuscript

411 two times less frequently in the central sulcus ($p<0.00001$); these two locations are highlighted in
412 blue in Figure 5A.
413
414 **KCs co-occur in channels across the cortex**
415 In order to determine whether KCs co-occur across the cortex, the KCs that were marked
416 independently on each channel were regrouped. Starting with the first KC latency, any KCs
417 occurring in other channels within the next 200ms were grouped as being part of the same KC
418 event. As the time delay of potential KC propagation across the cortex is unknown, this 200ms
419 time window was defined for grouping a KC event because it is the approximate time delay
420 reported for the slow oscillation from anterior to posterior scalp EEG recording sites (Massimini
421 et al., 2004). Each KC event, therefore, would minimally contain one channel and could
422 maximally contain the number of channels analyzed for an individual subject.
423 To examine if KC peaks in different channels participating in a KC spanned the entire 200ms
424 window, the time between the first and last peak in each KC containing more than one channel
425 was calculated. The mean and standard deviation of these maximum peak delays was calculated
426 for each night for each subject. All subjects showed a mean peak difference of less than 100ms
427 (Table 2). The single exception was one night for subject 9, where only one KC involved both
428 channels; as a result, the mean only reflects one calculation. Therefore, even though a 200ms
429 window was chosen to include KCs potentially traveling across the cortex, KCs occurred in
430 almost all cases in less than half this time.
431 To test whether these observed KC co-occurrences were significant, we simulated a set of
432 expected KC data under the null hypothesis that the KC times are unrelated in different channels.
433 This expected distribution was created by randomizing the inter-KC intervals within channels of

eNeuro Accepted Manuscript

the observed KCs and grouping the latencies over channels within 200ms windows, as was done with the observed KCs. We examined observed and expected KCs occurring in one channel versus two or more channels for each subject (Figure 6). In the observed KCs, there are KCs which only occur in one channel (Figure 6A, light orange). However, there are many more KCs which only occur in one channel for the null distribution (Figure 6B, light purple). Conversely, there is a larger number of KCs involving two or more channels for the observed data (Figure 6A, dark orange) than under the null hypothesis (Figure 6B, dark purple). To statistically verify this observation, a Fisher's exact test was performed, comparing the number of observed KCs to the null-distribution in one channel versus two or more channels. For 20 nights over eight subjects, this was highly significant ($p<0.05$, Bonferroni corrected) (Table 3). For four nights over two subjects (three out of four nights for one subject and one out of three nights for the other subject), it was not. Due to the variable number of channels for each subject, the 'one channel' versus 'two or more channels' was the only comparison testable for all nine subjects. In eight subjects, it was possible to repeat this test using expected and observed data for one channel and three or more channels; for seven of these subjects at least one night was significant at $p<0.05$ Bonferroni corrected, while the night of the eighth subject was not significant. For six subjects it was possible to test up to four or more channels; in this case, we find all nights for five subjects to be significant at $p<0.05$ Bonferroni corrected and not in one night in one subject. This analysis demonstrates that KCs co-occur across the cortex.

KCs do not occur in particular sequential order across the cortex

As examined above, channels participating in a KC event exhibit a tighter time window than the 200ms used to group KC events. However, this specific limit was imposed to investigate

eNeuro Accepted Manuscript

propagation sequences: according to Massimini et al. (2004), it takes approximately 200ms for a slow wave to travel from anterior to posterior cortex. As stated previously, because the potential propagation time of KCs is unknown, the time delay of the SO was used as a maximum time window. To test the hypothesis that KCs occur in a sequential order across the cortex, we performed a multinomial test on the sequential order of channels participating in the observed KCs. Using the KC peak latencies, we recorded for a pair of channels the number of times the KC peak occurred in channel A before channel B and the number of times the KC peak occurred in channel B before channel A. In this example of two channels, the multinomial test determined when one sequential order occurred significantly more often than the other sequential order. Out of 341 channel pairs tested over a representative night for each of the nine subjects, only 20 pairs from two subjects (subjects two and six) were statistically significant at $p<0.05$ after Bonferroni correction. These results indicate that when two channels repeatedly record KCs within a 200ms time window, only 6% of these 341 channel pairs show a significantly consistent latency order. Conversely, 94% of channel pairs show no systematic latency even though they occur repeatedly within the same trans-cortical KCs.

If KCs significantly occurred in a sequential order from anterior to posterior cortex, we would expect to find ordered sequences of two or more channels beginning in anterior cortical regions and finishing in posterior cortical regions. Thus, we examined individually all of the electrode-pairs to determine if they were systematically engaged in an anterior to posterior direction. We found that for subject two, 11 out of the 16 significant pairs started in various parts of cortex and ended in the temporal lobe. Three other pairs were situated along the same electrode, one was a pair of mirrored locations across the hemispheres, and the last was a pair with a slight posterior to anterior direction (Figure 7B, red arrows). Of the four significant pairs found for subject six,

eNeuro Accepted Manuscript

480 there was evidence of anterior to posterior propagation for three pairs, all lying entirely within
481 prefrontal cortex. One of these three pairs was along the cingulate gyrus. One other pair was
482 located along the same electrode, with no anterior-posterior separation.
483 We further tested three, four, and five channel sequences, whenever possible given the number
484 of channels and the rate of multi-channel KC occurrence for each subject. Out of 222 triplets
485 tested, 5 from subject six were statistically significant at $p<0.05$ after Bonferroni correction. As
486 with the pair results for this subject, these triplets showed anterior to posterior propagation only
487 within the prefrontal cortex, as well as patterns that bounced back and forth or looped around
488 within the frontal cortex. There were no significant sequences involving four or five channels.
489
490 **Automatic template-based detection of KC-like activity**
491 The above analyses were performed on the manually-marked KCs. The strict criteria used to
492 select these phenomena, most notably that there was a flat baseline (i.e. no preceding oscillation)
493 prior to the KC, may have prevented KC-like phenomena from being detected, and thus result in
494 an underestimation of the degree of KC co-occurrence. In order to detect KC-like events, a
495 template was created for each channel and applied at the times of manual KCs occurring in at
496 least one channel (Figure 8). A threshold was established as the 99th percentile of periods when
497 no KC was visually present. Events which exceeded the template threshold were included as KC-
498 like events (see Materials & Methods). Application of these individualized channel templates
499 identified 13,383 KC-like events—a 96.8% increase in detected KCs—and 98.7% of the 13,821
500 manually marked KCs.
501 Compared to the manually-detected KCs, template-detected KCs were smaller in amplitude
502 (manual = 420±219μV versus template = 326±183μV) and had more variance in the pre-KC

eNeuro Accepted Manuscript

period (manual KCs=1945±1604 versus template-detected 7388±10,708). The variance in the pre-activity period (Figure 9A) and the KC peak amplitude (Figure 9B) for each of subject 1's four channels are plotted for the null times (black distribution), manual KCs (red distribution), and template-detected KCs (blue distribution). In some cases, the template-detected KCs were smaller in amplitude than the manual KCs, without much distinction in the variance (Channel 1), while in other cases, the opposite occurred: the variance was larger for template-detected KCs than manual KCs, without a large distinction in amplitude (Channel 4). In most cases, it was a combination of variance and amplitude that distinguishes the manual and template-detected KCs (Channels 2 and 3).

In order to evaluate for all channels the contributions of KC peak amplitude and pre-KC period variance in distinguishing manual from template-detected KCs, Z scores were calculated for the KC peak amplitude and pre-KC period variance for each channel with respect to the null values (Figure 9C; an expansion of the lower left corner outlined in grey in Figure 9C is presented to the right). In general, as above, the manual KCs (red circles) are larger in amplitude (i.e. shifted to the right on the x-axis) than the template-detected KCs (blue triangles). The manual and template-detected values for each channel are connected by a line. This line is green if the manual KCs were larger in amplitude than the template-detected KCs; however, this line is black in the rare cases where the template-detected KCs are larger in amplitude than the manual KCs. Furthermore, the pre-KC period variance is generally larger (i.e. shifted up on the y-axis) for the template-detected KCs compared to the manual KCs within each channel. To test these observations, a paired t-test between the manual and template-detected KC z-transformed amplitudes over all channels was significant ($p=0.000065$), as was a paired t-test between the z-transformed variance in the pre-KC period for manual and template-detected KCs over all

eNeuro Accepted Manuscript

channels ($p=0.00027$). While there are clear overall distinctions in amplitude and pre-KC period variance between template-detected and manually-marked KCs, they appear to form a continuum on a channel-by-channel basis, and thus both manual and template-detected KCs should be considered together when examining the true extent of cortical involvement at the time of KCs. We further examined whether a directionally-consistent temporal lag existed between manually-detected and template-detected KCs by subtracting the average of the template KC peaks from the average of the manual KC peaks within each KC event. The mean lag was -1.25ms with a standard deviation of 40ms and the normality of the distribution was determined visually; therefore, we concluded that no such temporal relationship existed between the manual and template KCs.

Including KC-like activity increases the multi-channel participation of KCs

Combining the number of manually marked KCs with the template KCs resulted in 27,204 total KCs over all subjects. We first examined how the addition of template KCs increased multi-channel participation. In subjects where all channels participated in a subset of manually marked KCs, the percentage of such KCs increased with the addition of template KCs (Figure 10A). Similarly, in subjects where only a subset of channels participated in manually marked KCs, the addition of template KCs resulted in KCs where all possible channels participated (Figure 10B). Manually-marked KCs already showed significant co-occurrence across the cortex; the addition of KC-like activity indicates that KCs co-occur even more broadly across the cortex.

In Subjects 1, 2, 3, and 9, all channels participated in a subset of manually marked KCs. For subject 1, the percentage of KCs involving all four channels increased from about two percent in the manual case to nine percent after addition of the template KCs. For subject 2 (Figure 10A),

eNeuro Accepted Manuscript

549 all 13 channels participated in only 0.7% of manual KCs, which increased to about five percent
550 of all KCs with the addition of KC-like activity. If 10 or more channels are considered as a
551 group for subject 2, then the percentage of total KCs increased from about four percent in the
552 manual case to 20% in the case of manual plus template KCs. For subject 3, the increase in KCs
553 involving all channels was slight, from one to 2.5%, while for subject 9, this increase was from
554 about three percent to about 28%. While this latter result indicates the largest increase, there are
555 only two channels for subject 9.
556 In subjects 4, 5, 6, 7 and 8, KCs with all channels participating were not found until template
557 KCs were included. In subject 4, only five out of seven channels maximally participate in
558 manually marked KCs, and these represent only 0.2% of KCs. With the addition of template-
559 detected KCs, KCs may now involve five, six, or seven channels, accounting for over 12% of all
560 of subject 4's KCs. For subject 5, manual KCs only maximally involve three out of five possible
561 channels, representing 0.6% of KCs. After template detections, about 38% of the subject's KCs
562 involve three, four, or five channels. For subject 6 (Figure 10B), only 2% of manually marked
563 KCs involve six out of seven channels. After template application, this increases to almost 20%,
564 and the number of KCs involving all seven channels is just under 11%. In subject 7, a maximum
565 of only five out of eight possible channels participate in manual KCs, and 86% of KCs only
566 involve one channel. After template detection, KCs involving six, seven, and eight channels
567 collectively account for about seven percent of KCs. For subject 8, only three out of four
568 channels maximally participate in the manual KCs, but after including KC-like activity, about six
569 percent of KCs include all four channels.
570 A 200ms detection window on manually marked KCs was chosen based on the differences in KC
571 peak latencies reported at the scalp for SOs (Massimini et al., 2004). However, if this window

eNeuro Accepted Manuscript

was artificially small, then we may have underestimated the true extent of KC co-occurrence. In order to test for this possibility, we re-calculated co-occurrence after grouping KCs using a 200ms 'crawl' window (Figure 10). In the analyses described above, we start at the first KC peak and search within the following 200ms window for any other manually marked KC peaks in other channels. In the 'crawl' analysis, we follow the same procedure, but shift the 200ms window to follow the second KC peak. The window continues to shift until there are no further detections within the 200ms window. The re-calculated co-occurrence histograms showed minimal changes using this procedure. Only three of the nine subjects (two, three, and six) showed an increase of more than one KC with participation of all channels. Even in these subjects, the effects were minimal as seen by comparing the red and gray bars in Figure 10. In contrast, adding template-detected KCs had a substantial effect on co-occurrence, as seen by comparing the red and blue bars in Figure 10.

In summary, including only the manually-marked KCs, most KCs (76%, average across all subjects) occurred in a single location, and rarely (1%) in all locations. However, if template-detected KCs were included, only 15% occurred in a single location and 27% in all locations.

After including KC-like activity, KCs are smallest in anterior prefrontal regions

In Figure 4B, average KC amplitudes, including both manual and template-detected KCs, are shown for each channel (color-coded by subject). For comparison, the same amplitude data for manual KCs only are plotted in Figure 4A. The addition of the template KCs generally decreases the average KC amplitude at each channel, as seen by a reduction in circle size between A and B, and as shown to be significantly different in Figure 9C.

eNeuro Accepted Manuscript

In order to compare the amplitude of KCs in different areas, a linear mixed effects model of the amplitudes was again performed. The anterior prefrontal channels were found to be ~30% smaller than the orbitofrontal reference channels ($p=0.045$, blue circle in Figure 4B). Again, this finding is in contrast to what would be predicted by scalp EEG.

Adding KC-like activity has minor effects on the pattern of KC occurrence rates across cortical locations

We next examined how the addition of KC-like activity influences the spatial distribution of KC occurrence rates across the cortex. Again, in Figure 5B, the average KC occurrence rate for each channel is color-coded by subject, including both manual and template-detected KCs, for comparison with the same occurrence rate data plotted for manual KCs only in Figure 5A. For each subject, the occurrence rate of KCs in each channel is normalized to the channel with the highest KC occurrence rate.

Similarly, in order to test if KC occurrence rate varies across locations after including template-detected KCs, a linear mixed effects model was again applied to the inter-KC intervals for each channel. Compared to the orbitofrontal reference, KCs still occur significantly more frequently in posterior cingulate (26% more, $p<0.00001$) and posterior prefrontal (6% more, $p=0.044$). They no longer occur more frequently in anterior cingulate or ventrolateral temporal cortex, but KCs now occur more frequently at the temporo-parieto-occipital junction (15% more, $p=0.048$). These groups are highlighted in pink in Figure 5B. As was the case with the manual KCs, the anterior prefrontal occur 26% ($p<0.00001$) and the central sulcus occur 48% ($p=0.0001$) less frequently than the orbitofrontal channels and are highlighted in blue in Figure 5B.

eNeuro Accepted Manuscript

Adding KC-like activity does not reveal any systematic sequential order across the cortex

We tested if using only manually marked KCs under-sampled KC activity and therefore, resulted in the apparent lack of any systematic sequential order of KCs across the cortex. This was achieved by repeating the analysis described above after the addition of the template KCs, where a multinomial test was used to identify channel pairs with significant sequential ordering. Due to the addition of so many more KCs, a total of 412 pairs of channels (as compared to 341 pairs in the manual only KCs) were tested over a representative night for all nine patients. Of these pairs, 33 pairs over four subjects were significant in addition to the pairs found using only manual KCs, for a total of 53 significant pairs (13%). Subjects one, four, eight, and nine did not show any significant pairs before or after the addition of KC-like activity. A single significant pair, from ventral to dorsal, was found in subject five after the addition of KC-like activity. Subject six did not add any additional pairs.

Subject three was one of the subjects for whom anterior to posterior propagation could be most clearly tested due to electrode placement in prefrontal and parietal cortices (Figure 7A). Of six prefrontal-parietal pairs examined, there were no significant pairs using only manual KCs, and even after the addition of KC-like activity, there was no evidence of significant frontal to parietal propagation; rather, there were two significant pairs found within frontal cortex. Subject seven did not have any significant manual pairs; however, one pair along the same electrode became significant after the addition of KC-like activity. Subject two already showed a large number of significant pairs (16) in testing manual KCs; the addition of KC-like activity added 29 significant pairs (Figure 7B). This subject shows a strong tendency for significant pairs, in fact 64% of such pairs, to lead to temporal cortex. Apart from this pattern, the other pairs show sequences in many directions within and between hemispheres. In addition to the 47 significant pairs plotted

eNeuro Accepted Manuscript

in Figure 7, there are only 6 other significant pairs over three subjects including both manual and KC-like activity that were significant and have been described above but are not plotted. While the addition of KC-like activity makes it more possible to see evidence of anterior to posterior propagation, frontal to parietal propagation still is not seen in the 8 contact-pairs in 3 subjects where it could be tested. Although propagation within the frontal lobe in various directions is seen, the only consistent propagation between lobes is from frontal to temporal.

Insular origin of KCs is not supported by intracranial recordings

In addition to the channel pairs which had a significant order of KC occurrence, we examined a specific prediction made in the literature regarding the typical origin of KCs. Murphy et al. (2009) interpreted scalp EEG as demonstrating that 46% of isolated SOs, i.e. KCs, originate in the insula. Using bipolar SEEG, we demonstrated insular generation of KCs in 2 contacts in 2 patients. Out of 1080 KC-events in these subjects, only 177 (16%) involved the insula. Thus, at least 84% of KC-events originated outside the insula. Of the KC-events that did include the insula, not all began in the insula. Specifically, of the 61 KC-events involving the insula and at least one other structure, the insula led in 38 KCs (62%). If we extrapolate this proportion to all insula KCs, then the proportion of all KCs led by the insula would be about 10% (62% of 16%). While our sampling of 2 insular contacts from 2 patients is small, the inference of Murphy et al. (2009) does not appear to be supported by direct intracranial recordings.

KCs may show a slight anterior to posterior propagation when all individual trials are tested

eNeuro Accepted Manuscript

662 In order to directly test the hypothesis that there is a significant distance versus delay relationship
663 between anterior and posterior cortex during the KC, we examined 6224 manual plus template
664 KCs that involved 51 pairs located along the anterior to posterior axis. To isolate anterior to
665 posterior propagation from lateral to medial propagation, selected pairs could only have one
666 contact separation in the medial to lateral direction. We found 3702 KC pairs where the peak
667 latency occurred first in the anterior channel followed by the posterior channel; in contrast, we
668 found only 2518 KC pairs that showed the opposite progression from the posterior to anterior
669 channel. This represents a ~47% increase of KCs in the anterior to posterior direction as
670 compared to the posterior to anterior direction. The remaining four pairs exhibited a 0ms delay.
671 The distance between these channel pairs was plotted as a function of the average KC latency
672 difference between them (Figure 11A, black circles & red triangles). Distance between channel
673 pairs was also plotted against the individual KC latency differences between them (Figure 11B,
674 black circles & red triangles). A linear mixed model regression found that a significant
675 relationship between anterior to posterior distance and delay existed across these pairs,
676 considering either the average KC latency difference (Figure 11A, purple line, $p=0.007$) or the
677 individual KC latency difference (Figure 11B, purple line, $p<10^{-4}$).
678 As we found that a large number of pairs in one subject exhibited a significant propagation from
679 prefrontal areas to temporal cortex, we examined the effect of eliminating these pairs, which are
680 plotted as red triangles in Figure 11. When these pairs are excluded, there are 2394 pairs which
681 progress from anterior to posterior and 2061 posterior to anterior pairs, which only represents a
682 16% increase in anterior to posterior pairs. The black circles in Figure 11 represent the non-
683 temporal pairs that were included in a subsequent linear mixed model regression, which did not
684 find a significant relationship between anterior to posterior distance and average KC latency

eNeuro Accepted Manuscript

differences (Figure 11A, green line, p=0.08); however, when KC latency differences were considered individually, a significant relationship again occurred (Figure 11B, green line, p=0.003).

In all cases, significant distance versus delay relationships explained only a small percent of the variance: 2% when all pairs are considered individually, 13% when the average KC latency differences for all pairs are used, or 0.2% when individual pairs, excluding temporal pairs, are considered.

The above analyses considered the relative anterior-posterior location of the two contact-pairs, in order to test the hypothesis that there is a global anterior to posterior propagation of KCs. This hypothesis predicts that anterior sites would precede posterior, and that the time delay would increase with increasing distance. We also tested the hypothesis that, regardless of direction, there is an overall distance versus delay relationship, by examining the absolute distances and absolute delays of all pairs. As the distribution is no longer normal, a regression could not be calculated. Instead, the correlation calculated between the absolute distance and absolute delay of these KC pairs was very small ($r=0.071$), although it was significant ($p=2.1e-08$). As a direct comparison, the correlation was also calculated between the signed distance and absolute delay, as modeled above. This correlation was again significant, and greater than that for absolute distance and absolute delay, but it was still small: $r=0.12$, $p<2.2e-16$.

In summary, there is a highly significant excess of KCs that propagate in the anterior to posterior direction as compared to the posterior to anterior, and the average delays between locations are related to the distance between them provided the frontal to temporal pairs are included. However, although this is true on a statistical basis, the variation between sites and individual KCs is very large, so this effect only explains a very small part of the observed pattern.

eNeuro Accepted Manuscript

Stage 2 and Stage 3 KCs have similar neurophysiological characteristics

In the above analyses, KCs were defined by their morphology and accompanying decrease in high gamma power, and thus were not confined to stage 2 sleep. In order to compare stage 2 (N2) and stage 3 (N3) KCs, sleep staging was performed on scalp electrodes for the patients from Massachusetts General Hospital and on SEEG for the patients from La Timone Hospital, where scalp EEG was unavailable. Unless otherwise noted, all analyses presented below were performed on the combined manual and template detected KCs. There were 2.8% fewer KCs added using template detection during N2 than N3, which was not significantly different when tested over all subjects using a paired t-test ($p=0.64$).

Averaged KC waveforms overlaid for N2 and N3 for subject one's four channels have indistinguishable morphologies (Figure 12A). To test if there is a statistically significant difference between N2 and N3 peak amplitudes, Z scores for N2 and N3 were calculated for the KC peak amplitude for each channel with respect to the null values. When tested, Z-scored amplitudes for N2 and N3 over all channels show no significant difference (paired t-test, $p=0.9$). To evaluate whether a difference in the high gamma drop that characterizes the downstate differs between N2 and N3, the Hilbert analytic amplitude for high gamma was calculated from 25ms before, to 25ms after, the KC peak at 0ms for all KCs. These values were averaged over all KCs in a channel, separately for N2 and N3. A paired t-test between the averaged N2 and N3 high gamma values over all channels found no significant difference ($p=0.34$).

In order to determine if manually marked N3 KCs more closely resemble a slow oscillation than N2 KCs, the pre-KC peak amplitude was detected within a -850 to -350ms window prior to the KC peak at 0ms and compared to the amplitude of this KC peak. Assuming that the up and

eNeuro Accepted Manuscript

731 downstate of a slow oscillation have the same amplitude but opposite polarities, a slow
732 oscillation would be implied if the pre-KC peak were equal to the KC peak. This was a more
733 direct measure of whether the KC was preceded by a slow oscillation upstate than the previously
734 used pre-KC variance measure, which tested overall variability and was not scaled to the
735 expected value of an SO. When the means over all KCs over all channels are calculated, the pre-
736 KC peak of both manual N2 and N3 KCs is equal to 26% of the KC peak; in comparison,
737 template-detected N2 KC means are 67%, while template-detected N3 KC means are 83%. If
738 the mode is calculated instead, pre-KC amplitude of manual N2 KCs are 19% of the KC peak,
739 compared to 22% for manual N3 KCs; again, this is much smaller than for the template-detected
740 KCs, which are 43% for N2 and 44% for N3. Therefore, the manually-detected KCs showed
741 similar pre-KC amplitudes regardless of sleep stage, which were much smaller than would be
742 expected for a slow oscillation and smaller than template-detected KCs.
743 To test for a difference in occurrence rate between N2 and N3, the average ISI for each stage for
744 each channel was calculated after applying a Box-Cox transform to normalize the data. Out of
745 all 55 channels, 32 channels (58%) occurred less frequently for N2 than N3. A one-tailed paired
746 t-test found that N2 KCs occur less frequently than N3 KCs ($p=0.003$). In summary, KCs in
747 stage 2 and 3 have very similar morphologies, pre-KC amplitudes, KC peak amplitudes, and
748 accompanying decrease in high gamma power. N3 KCs occurred more frequently than N2 KCs.
749
750 **KCs in N2 and N3 do not differ in the number of participating channels.**
751 A separate Chi-squared test was performed for each subject, comparing the number of KCs
752 occurring in N2 and N3 over each number of channels participating in a KC (i.e. one channel up
753 to the maximum number of channels recorded for that subject). For the majority of subjects

eNeuro Accepted Manuscript

754 there was no significant difference between N2 and N3 KCs in terms of multichannel
755 participation: subject 1 (p=0.055); subject 2 (p=0.077); subject 3 (p=0.068); subject 4 (p=0.061);
756 subject 5 (p=0.78); subject 7 (p=0.97); and subject 8 (p=0.38). While some of these values are
757 close to reaching significance, there is no clear pattern of one stage involving more or less
758 channels than the other stage. As an example of this, Subject 4 is presented in Figure 12B with
759 the percentage of KCs occurring in each number of channels by stage, with N2 plotted in red and
760 N3 in blue. For two subjects, there was a significant difference between the distribution of
761 channels participating in N2 and N3 KCs: subject 6 (p=0.011) and subject 9 (p=0.000056). In
762 both cases, the distribution of N2 KCs is skewed to the right, indicating that N2 KCs involve a
763 greater number of channels than N3 KCs for that subject. The percentage of KCs occurring in
764 each number of channels by stage for these two significant subjects is plotted in Figure 12B.
765 These results could indicate that there is a greater co-occurrence of a KC across locations during
766 N2 as compared to N3. Subject 9, however, only involved two channels, and therefore, it is
767 difficult to predict whether this relationship would remain with the addition of more channels.
768 The results for the other subjects that did not reach significance also exhibited variable patterns,
769 some with slightly more multi-channel KCs in N2, and others in N3, or neither. Thus, if there is
770 a difference between stages in multi-channel participation, it is weak.
771
772 **KCs in N2 and N3 do not differ significantly in their propagation sequences**
773 As described above, a significantly consistent direction of propagation between each pair of
774 bipolar recordings was detected using binomial tests. Since the power of the binomial test is
775 critically dependent on the number of observations, we subsampled the N2 or N3 data in any
776 given patient so that the number of KC events was equal for the two sleep stages. With the

eNeuro Accepted Manuscript

much-reduced power, the number of significant pairs was only 39 for N2 and 27 for N3, without Bonferroni correction, out of 180 bipolar pairs (Chi-square=2.67, df=1, p>.10). Due to the small number of remaining events after balancing N2 and N3 in each subject, we are unable to draw any strong conclusions regarding whether the patterns of sequences are significantly different in N2 or N3.

In summary, the similarities and differences between N2 and N3 KCs support the hypothesis that physiological and morphological properties define the KC, rather than their occurrence during a particular stage. For the majority of subjects, there was no difference in multichannel participation between stages, while findings regarding propagation patterns were inconclusive. We conclude that the defining physiological and morphological characteristics of a KC do not differ between N2 and N3 and therefore, that global KC properties may be studied collapsed between stages.

Summary of Current Results

Figure 13 depicts a summary of our findings in contrast to current views. Based on scalp EEG and MEG, as well as referential intracranial recordings, a monolithic interpretation of KCs (or their equivalent, isolated SOs) has been put forth wherein KCs are generated initially and most strongly in prefrontal cortex (Figure 13A, orange star), and then propagate consistently to parietal cortex (blue arrow & fading orange background). In contrast, our results demonstrate that KCs are smallest in anterior prefrontal areas (Figure 13B, orange star), that they arise all over the cortex (additional stars), and may co-occur across many areas, as represented by the uniform yellow background. While there is a weak overall tendency for KCs to propagate posteriorly, especially from frontal to temporal sites (grey arrow), KCs seldom exhibit a

eNeuro Accepted Manuscript

consistent pattern of propagation between any two cortical locations (groups of colored arrows). Furthermore, the current results show that while some KCs involve widespread cortical locations, others can be very focal. In summary, our results suggest that each KC may be unique in its origin, extent and spread.

Discussion

Although KCs have been studied for over 80 years, their origin and spread remain controversial. Do they occur quasi-synchronously in widespread cortical areas (Mak-McCully et al., 2014), or arise in midline frontal areas and spread parietally (Massimini et al., 2004)? Are KCs a fundamental cortical process, or are some cortical areas unable to generate KCs (Wennberg, 2010)? In locations generating KCs, are their amplitudes and occurrence rates uniform? These issues remain controversial because previous studies used methods which provide ambiguous localization. We examined the spatial and temporal relationships of individual KCs recorded simultaneously in multiple cortical locations using bipolar SEEG recordings, validated with HGP. Using this unambiguous method, we found that KCs can be generated throughout the cortex, including areas previously asserted not to generate KCs: the cingulate, ventral temporal, and occipital cortices. Contrary to previous accounts, KCs were smallest in anterior prefrontal areas. A given KC may occur in only one sampled location, or may co-occur in widespread cortical sites. When KCs were absent in other channels, KC-like activity were often found. Regardless of whether this KC-like activity was included, most channel pairs did not show a regular propagation direction. However, there was a weak statistical tendency favoring anterior to posterior propagation. We conclude that KCs have multiple degrees of freedom which may support the spatiotemporal patterns underlying memory consolidation and cortical restoration.

eNeuro Accepted Manuscript

Methodology for obtaining unambiguous generator localization

Previous examinations of KCs in humans utilized EEG, MEG, EEG with fMRI, ECOG, or referential SEEG. In contrast, our study utilized bipolar SEEG derivations, where one contact was immediately above the local cortical surface, and one in the immediately subjacent white matter. We validated KCs by demonstrating an accompanying statistically significant drop in HGP. Thus, unlike previous studies, we could be certain of local generation at the electrode site. Dense microelectrode array recordings demonstrate that the KC is a cortical downstate, with a cessation of neuronal firing and broadband decrease in spectral power of the local field potential (LFP), due to inward apical dendritic currents in layers 2/3 (Cash et al., 2009). The current return is in layer 1, resulting in a surface negativity in ECOG or SEEG. Ambiguities arise because each sensor records the summation and cancelation of all cortical potentials. Although distant areas contribute to the LFP inversely according to the square of their distance (Linden et al., 2011), their total contribution may exceed that of local sources when much of the cortex is active (Klee and Rall, 1977).

All potential measurements are relative to a reference electrode, and the above comments assume an inactive reference. However, when generators are distributed, it is difficult to confirm that a reference electrode location is inactive. Extracranial references cannot be assumed to be inactive because the amplitude of distributed generators declines little from cortex to scalp (Cooper et al., 1965). Average references are not neutral unless all sides of the volume conductor are equally and densely sampled, a practical impossibility due to the neck and face, and to scalp incisions. Thus, even locally-recorded potentials with ECOG and SEEG are difficult to interpret as definitively reflecting only locally-generated activity.

eNeuro Accepted Manuscript

Bipolar transcortical SEEG derivations are insensitive to distant sources because the two contacts act as references for each other. The positive and negative peaks of the locally-generated KC are determined by the separation between the generating transmembrane inward and outward currents, measured to be separated by ~1mm (Cash et al., 2009). The two leads in the bipolar SEEG pair were separated by 2.6 to 5.6mm, enabling them to capture the entire local field. In contrast, volume-conducted potentials from distant generators change little between the leads, and thus are removed by recording the difference between the leads. In addition, our KCs were accompanied by a suppression of broadband HGP, which has been observed to be highly focal (Lachaux et al., 2005), due to asynchronous generators (Linden et al., 2011). Thus, the co-occurrence of HGP suppression provides a strong confirmation of local KC generation.

The ambiguities resulting from the superposition of volume conducted potentials from many locations is much more severe for extracranial (scalp) EEG, where all locations are distant and the intervening skull and subcranial CSF further spread the potential (Ahlfors et al., 2010; Irimia et al., 2012). Inverse solutions use the pattern of potentials across sensors to infer possible generators. However, the inverse problem is mathematically ill-posed unless unproven assumptions are made. Scalp EEG also has a reference that is likely to be active. MEG does not use a reference, and is not smeared by the skull or CSF, but it also suffers from an irretrievably ambiguous inverse problem due to superposition of multiple sources at the sensors (Liu et al., 2002). While PET and fMRI provide unambiguous localization, and can be triggered by KCs recorded by simultaneous EEG, they lack the temporal resolution to determine if the activity they locate is due to the KC itself or to other time-locked activity.

Slow oscillations, and to a limited extent, KCs, have also been examined in animals. SOs occur synchronously over long distances in anaesthetized (Volgushev et al., 2006), and naturally

eNeuro Accepted Manuscript

869 sleeping cats (Destexhe et al., 1999), as do KCs (Amzica and Steriade, 1998). SOs are also
870 synchronous in anesthetized rats (Isomura et al., 2006). In contrast, SOs in ferret slices propagate
871 slowly (Sanchez-Vives and McCormick, 2000). Besides the effects of anesthesia and the loss of
872 synaptic connections in slices, the brain volume of humans is ~750 larger than rats and ~45 times
873 larger than cats (Haug, 1987), making the problem of synchronization or propagation different.
874 In summary, the recordings reported here better characterize KC origin and spread because they
875 were less prone to the ambiguities inherent to previous methods. However, electrodes were
876 placed for localizing seizures in patients with long-standing epilepsy. Epilepsy can be caused by
877 many factors, including a widespread genetic alteration in excitability which could affect the
878 occurrence, amplitude or spread of KCs. Conversely, the epilepsies of the patients studied here
879 were localized and non-genetic. Rarely, KCs have been noted to be altered in partial epilepsy:
880 KC rate increases, and elevated amplitude KC-like phenomena precede some seizures in
881 refractory nocturnal frontal lobe epilepsy (Si et al., 2010); however, none of the patients
882 analyzed here have this type of epilepsy. KC-like phenomena have occasionally been associated
883 with epileptiform spikes in temporal lobe epilepsy (Geyer et al., 2006), but would have been
884 identified and eliminated from the KCs studied here. Furthermore, we minimized possible
885 confounding effects of epileptiform activity by excluding all contacts in regions implicated in the
886 subject's epilepsy, and all epochs showing any signs of epileptic activity. Nonetheless, we cannot
887 completely exclude the possibility that the patient's epilepsy affected our results.
888 Since clinical considerations dictated electrode placement, we were also limited in the cortical
889 areas sampled, which differed in number and location between patients. Recordings also
890 differed in electrode contact spacing and the geometric relationship of the contact to the local
891 anatomy. This variability was addressed with linear mixed effects models which assume no

eNeuro Accepted Manuscript

892 interaction between patient and electrode location. If a patient's epilepsy type were to
893 differentially influence the size of KCs in different locations, then this assumption would be
894 violated. Overall, dense sampling in a larger number of patients would further disentangle the
895 multiple influences on KC origin, amplitude, occurrence and spread.
896
897 **KC generator localization**
898 Previous studies of KC generation have yielded a variety of localizations. Inverse solutions
899 applied to MEG or scalp EEG estimate KC generators to deep locations in the parietal lobe (Lu
900 et al., 1992), the sylvian fissure (Iramina and Ueno, 1996), midline structures (Murphy et al.,
901 2009; Wennberg and Cheyne, 2013), or deep in the parietal lobe or other variable deep locations
902 (Numminen et al., 1996). These results are often inconsistent with each other, and, overall, with
903 our results. For example, consistent with our findings, Wennberg and Cheyne (2013) estimated
904 KC generators to subcallosal or cingulate cortices. However, they are only two of many
905 generators, EEG and MEG estimates did not agree, and other generators localized in this study
906 were clearly incorrect, as they acknowledge. Murphy et al. (2009) estimated scalp EEG isolated
907 SO downstate (i.e. KC) generators mainly to the anterior cingulate, with secondary inferior
908 frontal gyrus, precuneus and insular generators, and no significant generation in many other
909 locations, which we demonstrate to generate KCs. The most parsimonious solution for most
910 inverse methods when applied to widespread generators is to estimate a relatively strong but
911 focal deep source.
912 Tones that evoke KCs also evoke increased BOLD in the superior temporal plane and F3op
913 (Czisch et al., 2009; Dang-Vu et al., 2011). However, these increases are likely to represent
914 BOLD activity related to the tone, rather than the KC, which is a downstate. During SOs, PET

eNeuro Accepted Manuscript

915 also shows a superior temporal increase, with a subcallosal decrease (Dang-Vu et al., 2005).
916 While the PET findings are during SOs, their location corresponds with some of the areas where
917 we demonstrated KC generation.
918 Wennberg (2010) investigated KC localization using average reference ECOG and SEEG in
919 humans and recorded the largest amplitude KCs in dorsal frontal areas, which he interpreted as
920 being the site of the largest KC generators. We demonstrate how average reference SEEG may
921 detect KCs in locations where they are not generated. In these sites, KCs are not seen in bipolar
922 SEEG and they do not correspond to a local drop in HGP. Thus, the presence or absence of KCs
923 in referential SEEG must be interpreted with caution. In contrast, we found that KCs in anterior
924 prefrontal regions are small and infrequent, while KCs occur more frequently in posterior
925 prefrontal cortex and posterior cingulate. We also demonstrate that KCs are generated in the
926 cingulate, ventral temporal, and occipital cortices, where Wennberg (2010) concluded that KCs
927 are not generated based on his failure to record them. Our data regarding ventral temporal sites
928 are not definitive because they were located in regions implicated in epileptogenesis.
929 Wennberg's (2010) emphasis on dorsolateral prefrontal generators may also have partially arisen
930 from his averaging of SEEG KCs at their frontal scalp EEG peak, while we identified KCs
931 individually at each cortical site.
932 Nir et al. (2011) demonstrated that unit-firing is correlated with SOs recorded in the medial
933 superior frontal gyrus, precuneus, anterior and posterior cingulate, entorhinal cortex, and
934 parahippocampal gyrus, thus demonstrating local generation. Although not specifically reported,
935 their data suggest that these locations also generate KCs. Using linear microelectrode arrays,
936 Cash et al. (2009) reported local transmembrane currents during KCs in prefrontal, lateral orbital,
937 middle and superior temporal, and supramarginal gyri. Using the same method, Csercsa et al.

eNeuro Accepted Manuscript

(2010) demonstrated local generation of SO in the postcentral and prefrontal cortices. These studies are consistent with our finding of locally-generated KCs in prefrontal, medioventral temporal, cingulate, orbital, and supramarginal cortices, and demonstrate or imply generation in the superior temporal and postcentral gyri, and the precuneus, where we failed to record. Overall, our findings combined with earlier studies demonstrate very widespread KC generation.

This conclusion is inconsistent with the studies described above which have been interpreted as indicating that large areas of cortex do not generate KCs. Using the more definitive methods described here, every location adequately sampled generated KCs, implying that KCs may represent a fundamental operating mode of human cortex. This conclusion raises the question of why KCs show significantly different amplitudes in different cortical locations. A complete answer cannot be given until the precise circuit and channel mechanisms of KC generation are better understood. However, different cortical areas vary considerably in their levels of particular ligand- and voltage gated channels, and associated proteins (Zilles et al., 2002; Hawrylycz et al., 2012); in particular, GABAb and potassium channels, which may be involved in KC generation (Cunningham et al., 2006; Kohl and Paulsen, 2010) .

KC propagation

Prior to this study, there has not been a rigorous examination of how KCs may propagate across the human cortex. In an influential study, Massimini et al. (2004) proposed that scalp EEG SOs in more posterior scalp sites peaked progressively later, with a delay of ~200ms, or a mean propagation speed of 2.5m/s. This view was extended by Murphy et al. (2009) in their analysis of isolated spontaneous SOs, i.e., KCs. Wennberg (2010), however, noted that KCs appeared to occur synchronously; when tested explicity (Mak-McCully et al., 2014), the observed delays in

eNeuro Accepted Manuscript

961 the peaks of averaged KCs between anterior and posterior sites in EEG, ECOG or SEEG were
962 about 10 times faster than had been previously predicted for isolated SOs (Massimini et al.,
963 2004; Murphy et al., 2009). Since averaging could obscure propagation patterns, we
964 systematically tested here for such patterns in single KCs. Again, we found scant evidence for
965 regular propagation patterns. When KCs occurred on different bipolar contacts within 200ms of
966 each other, they were tested to determine if their order of occurrence was significantly different
967 from chance. This occurred in only 6% of manually-detected KCs, or 13% when template-
968 detected KCs are also included. Several cases of significant propagation were observed within
969 the frontal lobe, including along the cingulate, where propagation could be in any direction.
970 Such complex patterns of propagation across the cortex have previously been noted by Hangya et
971 al. (2011). Frontal to parietal propagation, however, occurred in none of the 8 pairs of bipolar
972 contacts where it could be tested. A preponderance of insular origin of isolated SOs, i.e., KCs
973 (Murphy et al., 2009), was also not supported by our data in the two patients where it could be
974 tested. The most common pattern of propagation was from lateral prefrontal to lateral temporal,
975 reminiscent of the regular SO propagation from medial frontoparietal to medial temporal lobe
976 locations found by Nir et al. (2011), who also failed to find regular propagation within the medial
977 frontoparietal sites. SO propagation from anterior to temporal regions for both medial and lateral
978 cortex was also found by Botella-Soler et al. (2012).
979 Notwithstanding these negative results, we found a highly significant excess of KCs that
980 propagate in the anterior to posterior direction as compared to the reverse, and that average
981 delays between locations are related to their spatial separation. Although this is true on a
982 statistical basis, the variation between sites and individual KCs is large, so this effect only
983 explains 2% of the observed pattern.

eNeuro Accepted Manuscript

KCs are not confined to stage 2

Sleep stages defined using scalp EEG do not necessarily indicate a uniform and synchronous participation by different brain areas. For example, sleep onset measured locally in the thalamus has been noted to occur before sleep onset is detected in scalp EEG (Caderas et al., 1982; Gucer et al., 1978) or locally in the cortex (Magnin et al., 2010). We have also observed that isolated KCs may occur in parietal areas while rhythmic slow oscillations occur in frontal areas. Thus, we rigorously detected locally generated KCs using LFPs and HGP, and then characterized them regardless of sleep stage. Post hoc analyses showed that pre-KC amplitude, KC peak amplitude, and high gamma characteristics did not differ between stages 2 and 3. However, KCs did occur more frequently in N3 than N2. Critically, the extent of KC cortical involvement does not appear to change between stages.

Functional implications of KC heterogeneity

In summary, this is the first study to not only characterize the local generation of KCs in human cortex, but to examine their variable amplitude and occurrence rate, co-occurrence across the cortex, and propagation (Figure 13). Although systematic propagation of KCs between cortical sites can be observed, these are rare and in most cases the patterns of propagation vary randomly from KC to KC. Similarly, although there is a slight overall tendency for more anterior sites to lead more posterior ones, this tendency only explains a minute proportion of the variance, again leading to the conclusion that successive KCs are highly heterogeneous. We show in this paper that KCs differ greatly not only in their propagation patterns, but also in which areas are engaged, even though all areas seem to generate some KC activity. It has previously been shown

eNeuro Accepted Manuscript

1007 that KCs can be universal and quasi-synchronous across widespread cortical sites (Mak-McCully
1008 et al., 2014). Here, we confirm this finding and show that KCs can also be highly focal, or
1009 intermediate. This conclusion was robust to different methods of clustering KCs across channels,
1010 and was strengthened when using template- as well as manually-selected KCs.
1011 KC heterogeneity may arise from different cortico-cortical or cortico-thalamic mechanisms
1012 underlying the KC. Recent work has reexamined the role of the thalamus in the production of
1013 SOs, long thought to be an exclusively cortico-cortico mechanism, and found the thalamus to be
1014 important for SO frequency (David et al., 2013) and synchrony (Lemieux et al., 2014).
1015 Additionally, disruption of spindling in the thalamus has been posited as a mechanism of quasi-
1016 synchronous KC generation (Mak-McCully et al., 2014). Variable involvement of thalamic
1017 versus cortical mechanisms may help account for variability in the location and spread of KCs.
1018 KC heterogeneity may also reflect differential engagement of different cortical areas during the
1019 preceding waking period (Huber et al., 2004). This modulation of KC distribution may reflect
1020 restorative or consolidation processes during sleep. The later function is supported by the
1021 correlation of increasing SOs with behavioral consolidation (Marshall et al., 2006). In rodents,
1022 KCs are associated with the replay of firing patterns in the hippocampus and neocortex (Ji and
1023 Wilson, 2007). The previous conception of KCs as monolithic in origin, extent and spread would
1024 offer little scope for KCs to support the consolidation of distinct memories. In contrast, our
1025 demonstration that individual KCs are highly variable in location and propagation could provide
1026 a substrate for memory consolidation processes to engage different cortical networks, or the
1027 same networks in different sequences.
1028
1029 References

eNeuro Accepted Manuscript

1030 Ahlfors SP, Han J, Lin FH, Witzel T, Belliveau JW, Hamalainen MS, Halgren E (2010)
1031 Cancellation of EEG and MEG signals generated by extended and distributed sources.
1032 Human brain mapping 31:140-149.
1033 Amzica F, Steriade M (1998) Cellular substrates and laminar profile of sleep K-complex.
1034 Neuroscience 82:671-686.
1035 Botella-Soler V, Valderrama M, Crepon B, Navarro V, Le Van Quyen M (2012) Large-scale
1036 cortical dynamics of sleep slow waves. PloS one 7:e30757.
1037 Box GEP, Cox DR (1964) An analysis of transformations (with discussion). JR Statist Soc B
1038 26:211-252.
1039 Caderas M, Niedermeyer E, Uematsu S, Long DM, Nastalski J (1982) Sleep spindles recorded
1040 from deep cerebral structures in man. Clin Electroencephalogr 13:216-225.
1041 Cash SS, Halgren E, Dehghani N, Rossetti AO, Thesen T, Wang C, Devinsky O, Kuzniecky R,
1042 Doyle W, Madsen JR, Bromfield E, Eross L, Halasz P, Karmos G, Csercsa R, Wittner L,
1043 Ulbert I (2009) The human K-complex represents an isolated cortical down-state. Science
1044 324:1084-1087.
1045 Colrain IM (2005) The K-complex: a 7-decade history. Sleep 28:255-273.
1046 Cooper R, Winther AL, Crow HJ, Gey Walter W (1965) Comparison of subcortical, cortical and
1047 scalp activity using chronically indwelling electrodes in man. Electroenceph clin
1048 Neurophysiol 18:217-228.
1049 Crespel A, Coubes P, Baldy-Moulinier M (2000) Sleep influence on seizures and epilepsy effects
1050 on sleep in partial frontal and temporal lobe epilepsies. Clinical neurophysiology :
1051 official journal of the International Federation of Clinical Neurophysiology 111 Suppl
1052 2:S54-59.

eNeuro Accepted Manuscript

1053 Csercsa R et al. (2010) Laminar analysis of slow wave activity in humans. Brain : a journal of
1054 neurology 133:2814-2829.
1055 Cunningham MO, Pervouchine DD, Racca C, Kopell NJ, Davies CH, Jones RS, Traub RD,
1056 Whittington MA (2006) Neuronal metabolism governs cortical network response state.
1057 Proceedings of the National Academy of Sciences of the United States of America
1058 103:5597-5601.
1059 Czisch M, Wehrle R, Stiegler A, Peters H, Andrade K, Holsboer F, Samann PG (2009) Acoustic
1060 oddball during NREM sleep: a combined EEG/fMRI study. PloS one 4:e6749.
1061 Dang-Vu TT, Desseilles M, Laureys S, Degueldre C, Perrin F, Phillips C, Maquet P, Peigneux P
1062 (2005) Cerebral correlates of delta waves during non-REM sleep revisited. NeuroImage
1063 28:14-21.
1064 Dang-Vu TT, Bonjean M, Schabus M, Boly M, Darsaud A, Desseilles M, Degueldre C, Balteau
1065 E, Phillips C, Luxen A, Sejnowski TJ, Maquet P (2011) Interplay between spontaneous
1066 and induced brain activity during human non-rapid eye movement sleep. Proceedings of
1067 the National Academy of Sciences of the United States of America 108:15438-15443.
1068 David F, Schmiedt JT, Taylor HL, Orban G, Di Giovanni G, Uebele VN, Renger JJ, Lambert
1069 RC, Leresche N, Crunelli V (2013) Essential thalamic contribution to slow waves of
1070 natural sleep. The Journal of neuroscience : the official journal of the Society for
1071 Neuroscience 33:19599-19610.
1072 De Gennaro L, Ferrara M, Bertini M (2000) The spontaneous K-complex during stage 2 sleep: is
1073 it the 'forerunner' of delta waves? Neuroscience letters 291:41-43.

eNeuro Accepted Manuscript

1074 Delorme A, Makeig S (2004) EEGLAB: an open source toolbox for analysis of single-trial EEG
1075 dynamics including independent component analysis. Journal of neuroscience methods
1076 134:9-21.
1077 Derry CP, Duncan S (2013) Sleep and epilepsy. Epilepsy & behavior : E&B 26:394-404.
1078 Destexhe A, Contreras D, Steriade M (1999) Spatiotemporal analysis of local field potentials and
1079 unit discharges in cat cerebral cortex during natural wake and sleep states. The Journal of
1080 neuroscience : the official journal of the Society for Neuroscience 19:4595-4608.
1081 Destrieux C, Fischl B, Dale A, Halgren E (2010) Automatic parcellation of human cortical gyri
1082 and sulci using standard anatomical nomenclature. NeuroImage 53:1-15.
1083 Diekelmann S, Born J (2010) The memory function of sleep. Nature reviews Neuroscience
1084 11:114-126.
1085 Dykstra AR, Chan AM, Quinn BT, Zepeda R, Keller CJ, Cormier J, Madsen JR, Eskandar EN,
1086 Cash SS (2012) Individualized localization and cortical surface-based registration of
1087 intracranial electrodes. NeuroImage 59:3563-3570.
1088 Geyer JD, Carney PR, Gilliam F (2006) Focal epileptiform spikes in conjuction with K-
1089 complexes. Journal of clinical neurophysiology : official publication of the American
1090 Electroencephalographic Society 23:436-439.
1091 Gucer G, Niedermeyer E, Long DM (1978) Thalamic EEG recordings in patients with chronic
1092 pain. J Neurol 219:47-61.
1093 Halasz P (2005) K-complex, a reactive EEG graphoelement of NREM sleep: an old chap in a
1094 new garment. Sleep medicine reviews 9:391-412.
1095 Hangya B, Tihanyi BT, Entz L, Fabo D, Eross L, Wittner L, Jakus R, Varga V, Freund TF,
1096 Ulbert I (2011) Complex propagation patterns characterize human cortical activity during

eNeuro Accepted Manuscript

1097 slow-wave sleep. The Journal of neuroscience : the official journal of the Society for
1098 Neuroscience 31:8770-8779.
1099 Haug H (1987) Brain sizes, surfaces, and neuronal sizes of the cortex cerebri: a stereological
1100 investigation of man and his variability and a comparison with some mammals (primates,
1101 whales, marsupials, insectivores, and one elephant). Am J Anat 180:126-142.
1102 Hawrylycz MJ et al. (2012) An anatomically comprehensive atlas of the adult human brain
1103 transcriptome. Nature 489:391-399.
1104 Huber R, Ghilardi MF, Massimini M, Tononi G (2004) Local sleep and learning. Nature 430:78-
1105 81.
1106 Iramina K, Ueno S (1996) Source estimation of spontaneous MEG activity and auditory evoked
1107 responses in normal subjects during sleep. Brain topography 8:297-301.
1108 Irimia A, Van Horn JD, Halgren E (2012) Source cancellation profiles of
1109 electroencephalography and magnetoencephalography. Neuroimage 59:2464-2474.
1110 Isomura Y, Sirota A, Ozen S, Montgomery S, Mizuseki K, Henze DA, Buzsaki G (2006)
1111 Integration and segregation of activity in entorhinal-hippocampal subregions by
1112 neocortical slow oscillations. Neuron 52:871-882.
1113 Ji D, Wilson MA (2007) Coordinated memory replay in the visual cortex and hippocampus
1114 during sleep. Nature neuroscience 10:100-107.
1115 Klee M, Rall W (1977) Computed potentials of cortically arranged populations of neurons.
1116 Journal of neurophysiology 40:647-666.
1117 Kohl MM, Paulsen O (2010) The roles of GABAB receptors in cortical network activity.
1118 Advances in pharmacology (San Diego, Calif) 58:205-229.

eNeuro Accepted Manuscript

1119 Lachaux JP, George N, Tallon-Baudry C, Martinerie J, Hugueville L, Minotti L, Kahane P,
1120 Renault B (2005) The many faces of the gamma band response to complex visual stimuli.
1121 NeuroImage 25:491-501.
1122 Lemieux M, Chen JY, Lonjers P, Bazhenov M, Timofeev I (2014) The impact of cortical
1123 deafferentation on the neocortical slow oscillation. The Journal of neuroscience : the
1124 official journal of the Society for Neuroscience 34:5689-5703.
1125 Linden H, Tetzlaff T, Potjans TC, Pettersen KH, Grun S, Diesmann M, Einevoll GT (2011)
1126 Modeling the spatial reach of the LFP. Neuron 72:859-872.
1127 Liu AK, Dale AM, Belliveau JW (2002) Monte Carlo simulation studies of EEG and MEG
1128 localization accuracy. Hum Brain Mapp 16:47-62.
1129 Lu ST, Kajola M, Joutsiniemi SL, Knuutila J, Hari R (1992) Generator sites of spontaneous
1130 MEG activity during sleep. Electroencephalogr Clin Neurophysiol 82:182-196.
1131 Magnin M, Rey M, Bastuji H, Guillemant P, Mauguiere F, Garcia-Larrea L (2010) Thalamic
1132 deactivation at sleep onset precedes that of the cerebral cortex in humans. Proceedings of
1133 the National Academy of Sciences of the United States of America 107:3829-3833.
1134 Mak-McCully RA, Deiss SR, Rosen BQ, Jung KY, Sejnowski TJ, Bastuji H, Rey M, Cash SS,
1135 Bazhenov M, Halgren E (2014) Synchronization of isolated downstates (K-complexes)
1136 may be caused by cortically-induced disruption of thalamic spindling. PLoS Comput Biol
1137 10:e1003855.
1138 Marshall L, Helgadottir H, Molle M, Born J (2006) Boosting slow oscillations during sleep
1139 potentiates memory. Nature 444:610-613.

eNeuro Accepted Manuscript

1140 Massimini M, Huber R, Ferrarelli F, Hill S, Tononi G (2004) The sleep slow oscillation as a
1141 traveling wave. The Journal of neuroscience : the official journal of the Society for
1142 Neuroscience 24:6862-6870.
1143 MATLAB (2009) version 7.9.0 (R2009b): The MathWorks Inc.
1144 Murphy M, Riedner BA, Huber R, Massimini M, Ferrarelli F, Tononi G (2009) Source modeling
1145 sleep slow waves. Proceedings of the National Academy of Sciences of the United States
1146 of America 106:1608-1613.
1147 Nakagawa S, Schielzeth H (2013) A general and simple method for obtaining R2 from
1148 generalized linear mixed-effects models. Methods in Ecology and Evolution 4:133-142.
1149 Nir Y, Staba RJ, Andrillon T, Vyazovskiy VV, Cirelli C, Fried I, Tononi G (2011) Regional slow
1150 waves and spindles in human sleep. Neuron 70:153-169.
1151 Numminen J, Makela JP, Hari R (1996) Distributions and sources of magnetoencephalographic
1152 K-complexes. Electroencephalography and clinical neurophysiology 99:544-555.
1153 Oostenveld R, Fries P, Maris E, Schoffelen JM (2011) FieldTrip: Open source software for
1154 advanced analysis of MEG, EEG, and invasive electrophysiological data. Computational
1155 intelligence and neuroscience 2011:156869.
1156 Pinheiro J, Bates D, DebRoy S, Sarkar D, R Core Team (2015) nlme: Linear and Nonlinear
1157 Mixed Effects Models. In, R package version 3.1-120 Edition.
1158 R Development Core Team (2004) R: A language and environment for statistical computing. In.
1159 Vienne, Austria: R Foundation for Statistical Computing.
1160 Riedner BA, Hulse BK, Murphy MJ, Ferrarelli F, Tononi G (2011) Temporal dynamics of
1161 cortical sources underlying spontaneous and peripherally evoked slow waves. Progress in
1162 brain research 193:201-218.

eNeuro Accepted Manuscript

1163 Sanchez-Vives MV, McCormick DA (2000) Cellular and network mechanisms of rhythmic
1164 recurrent activity in neocortex. Nature neuroscience 3:1027-1034.
1165 Si Y, Liu L, Li Q, Mu J, Tian LY, Chen JN, Zhou D (2010) Features of the K-complex waves in
1166 refractory nocturnal frontal lobe epilepsy. Epilepsy research 92:219-225.
1167 Silber MH, Ancoli-Israel S, Bonnet MH, Chokroverty S, Grigg-Damberger MM, Hirshkowitz M,
1168 Kapen S, Keenan SA, Kryger MH, Penzel T, Pressman MR, Iber C (2007) The visual
1169 scoring of sleep in adults. Journal of clinical sleep medicine : JCSM : official publication
1170 of the American Academy of Sleep Medicine 3:121-131.
1171 Steriade M (2005) Sleep, epilepsy and thalamic reticular inhibitory neurons. Trends in
1172 neurosciences 28:317-324.
1173 Tononi G, Cirelli C (2014) Sleep and the price of plasticity: from synaptic and cellular
1174 homeostasis to memory consolidation and integration. Neuron 81:12-34.
1175 Volgushev M, Chauvette S, Mukovski M, Timofeev I (2006) Precise long-range synchronization
1176 of activity and silence in neocortical neurons during slow-wave oscillations [corrected].
1177 The Journal of neuroscience : the official journal of the Society for Neuroscience
1178 26:5665-5672.
1179 Wennberg R (2010) Intracranial cortical localization of the human K-complex. Clinical
1180 neurophysiology : official journal of the International Federation of Clinical
1181 Neurophysiology 121:1176-1186.
1182 Wennberg R, Cheyne D (2013) On noninvasive source imaging of the human K-complex.
1183 Clinical neurophysiology : official journal of the International Federation of Clinical
1184 Neurophysiology 124:941-955.

eNeuro Accepted Manuscript

1185 Zilles K, Palomero-Gallagher N, Grefkes C, Scheperjans F, Boy C, Amunts K, Schleicher A
1186 (2002) Architectonics of the human cerebral cortex and transmitter receptor fingerprints:
1187 reconciling functional neuroanatomy and neurochemistry. European
1188 neuropsychopharmacology : the journal of the European College of
1189 Neuropsychopharmacology 12:587-599.

1190

1191 Figure/Table Legends

1192 Table 1. Demographic and clinical information for all patients studied.

1193 Figure 1. Bipolar SEEG contacts. A. Bipolar SEEG contacts, color-coded by subject, are
1194 marked by circles on the medial (left) and lateral (right) surfaces of the brain. Bipolar SEEG
1195 contacts are grouped into one of 10 anatomical groups, as demarcated by black circles and/or one
1196 of the following labels: ac (anterior cingulate and subcallosal); af (anterior prefrontal cortex); pc
1197 (posterior cingulate); pf (posterior prefrontal cortex); cs (central sulcus); in (insula); f3op
1198 (inferior frontal gyrus; pars opercularis); of (orbitofrontal cortex); tp (temporo-parieto-occipital
1199 junction); vt (ventrolateral temporal cortex). B. Example SEEG electrodes for subject 1 (green)
1200 and subject 4 (purple) are superimposed on the subjects' MRIs. The arrows indicate the location
1201 of the bipolar contact pair chosen on each electrode. From the MRI, it is possible to see that the
1202 two contacts in each pair are spanning the local cortical mantle.

1203 Figure 2. Example KC localizations, waveforms, and downstate confirmations. KCs are plotted
1204 from representative sites across the cortical areas sampled. Individual KCs for each bipolar
1205 location are plotted in black with the average KC overlaid in red. The number of individual KCs
1206 plotted is listed above the waveforms. Below the KC waveforms, time frequency plots from 5-
1207 120Hz with a -1.5 to -0.5 second baseline relative to the most negative peak of the KC at time

eNeuro Accepted Manuscript

zero indicate a significant drop ($p<0.01$, uncorrected) in high gamma power at the time of the KC. Arrows indicate the bipolar locations where the plotted waveforms and time frequency plots were recorded. Circles indicate the subject color-coded bipolar channel locations, as in Figure 1. The four additional red squares indicate sites where KCs were located, but not included for additional analysis because they were part of an epileptic region or potentially in entorhinal cortex.

Figure 3. Bipolar versus common average reference recordings. Bipolar KC recordings (blue waveforms) were compared to monopolar KC recordings (red waveforms) referenced to a common average reference (T3, T5, F3, C3, P3, O1, F4, C4, P4, O2, T4, and T6) as in Wennberg (2010). Two pairs of adjacent contacts located on the same electrode of subject 4 were examined. A. Bipolar (blue) and referential (red) recordings from two adjacent contacts, both located in the white matter, as confirmed by MRI. Bipolar recordings show no KC but referential recordings do, despite the fact that no decrease in high gamma power is present in the time-frequency plots below each waveform. Thus, referential recordings show KCs even when they are not locally generated. B. Bipolar (blue) and referential (red) recordings from two adjacent contacts which span the gray matter, as confirmed by MRI. Both bipolar and referential recordings show KCs, together with decreased high gamma power. All recordings were averaged with respect to the peaks of KCs identified in the bipolar recordings in B.

Figure 4. KC amplitudes vary across the cortex. A. Average amplitude of manual KCs at each channel, color coded by subject, is highly variable across the cortex. However, no significant effects are found when a linear mixed effects model is applied. B. Addition of KC-like activity shows a similar pattern, but with the increased sample, the same linear mixed effects model now finds that the anterior prefrontal channels highlighted by the blue circle are ~30% smaller than

eNeuro Accepted Manuscript

1231 the orbitofrontal reference (p=0.045). Black circles in the top right indicate the amplitude scale
1232 represented by the size of each circle.
1233 Figure 5. KC occurrence rates vary across the cortex. A. Manually marked KCs color coded for
1234 each subject. The size of the circle indicates the KC occurrence rate at each location, normalized
1235 to the maximum KC occurrence rate seen on any channel for that subject. Black circles in the
1236 top right indicate this normalized occurrence rate scale. Locations identified by a linear mixed
1237 effects model to have a significantly higher occurrence rate than the orbitofrontal reference are
1238 highlighted by pink circles. Locations identified as occurring significantly less frequently are
1239 highlighted by blue circles. B. KC-like activity in addition to manually marked KCs. The
1240 locations showing a lower occurrence rate are the same as in A. The locations showing a higher
1241 occurrence rate differ with the addition of the template-detected KCs.
1242 Table 2. Mean and standard deviation of maximum KC peak differences between manually
1243 chosen KCs for each night for each subject.
1244 Figure 6. Observed manual KCs versus those expected under the null hypothesis of independent
1245 occurrence, for representative nights for each subject. A. KC events observed for each subject
1246 were classified into two groups: KCs with one participating channel (light orange) and KCs with
1247 two or more participating channels (dark orange). B. KC events derived from simulating an
1248 expected distribution for each subject were classified into the same two groups: one channel
1249 (light purple) and two or more channels (dark purple). For all subjects, there are more KCs that
1250 only occur in one channel expected under the null hypothesis than were actually observed.
1251 These distributions are tested statistically using a Fisher's exact test and these results are listed in
1252 Table 3.

eNeuro Accepted Manuscript

1253 Table 3. Fisher's exact test for co-occurrence for one channel and two or more channels; three or
1254 more channels; four or more channels; and five or more channels for all nights for all subjects.
1255 Bonferroni correction at $p<0.05$ was applied across all tests.

1256 Figure 7. Lack of systematic sequential order in KCs. Sequence pairs that are significant with
1257 manually marked KCs are plotted with red arrows, while sequence pairs that are only significant
1258 after the addition of KC-like activity are plotted with blue arrows. Sequence pairs tested but not
1259 significant are plotted in yellow. A. Subject 3 has electrodes in frontal and parietal cortices, but
1260 only shows significant sequences within the frontal lobe, and only after the addition of KC-like
1261 activity. B. Subject 2 shows a large number of significant sequence pairs (16) in manually
1262 marked KCs, the majority of which lead to the temporal lobe (11). This pattern is strengthened
1263 with the addition of KC-like activity (18 out of 29 additional significant pairs). A variety of
1264 other significant sequences are seen within the frontal lobe.

1265 Figure 8. Template application to detect KC-like activity. Channel-specific templates were
1266 created for each subject by averaging from -350ms to +650ms on the most negative peak at time
1267 zero over the manually detected KCs in each channel (box at left). The channel specific
1268 templates were then applied when a manually marked KC occurred in at least one channel. The
1269 templates were applied from -450 to +750ms, with time zero representing the average time
1270 between the first and last manually chosen channel peaks within a KC. Four such examples from
1271 subject 6 are plotted vertically. Manually marked KCs are plotted in red. The maximum value
1272 of the sliding inner product between the signal and the template was taken over the blue
1273 highlighted window. If the value was above the 99^{th} percentile of the null distribution for that
1274 channel and corresponded to the largest (or smallest) peak over the entire 1200ms window, the

eNeuro Accepted Manuscript

KC was recorded as KC-like activity (KCs in blue) and if it was below threshold, it was not (signal in black).

Figure 9. Manual KCs have smaller pre-KC period variance and larger amplitude than template-detected KCs. A. The probability density of variance in the pre-KC period (-1.4 to -0.4 seconds prior to peak) is plotted for the null times (black), manual KCs (red), and template-detected KCs (blue) for each of subject 1's four channels. B. The KC peak amplitude probability density of null times (black), manual KCs (red), and template-detected KCs (blue) are plotted for the same four channels as in A. C. For each channel, the manual (red circles) and template-detected (blue triangles) Z scores were calculated for the KC peak amplitude and the pre-KC period variance referenced to the null values. A line connects the manual and template-detected values for each channel. A green line indicates that the amplitude of template-detected KCs is smaller than that of manual KCs in that channel; a black line indicates the opposite relationship. On the right is an expansion of the lower left corner, which is outlined by a grey box.

Figure 10. Including KC-like activity increases multi-channel KC participation. The addition of KC-like activity (blue columns) to the manually marked KCs (red columns) increased the number of channels that were participating in KCs for all subjects. A. In subjects where a small number of manually marked KCs included the participation of all channels, the addition of KC-like activity increased the percentage of such KCs. B. Subjects that did not show maximum channel participation with manually marked KCs displayed KCs that included all channels after the addition of KC-like activity. In subjects two and six (pictured), and subject three (not pictured) the classification of KCs using a 200ms 'crawl' window slightly shifted the distribution of manual multi-channel participation to the right (grey columns), but not to the extent of the addition of KC-like activity (blue columns).

eNeuro Accepted Manuscript

Figure 11. Anterior to posterior contact pair distance versus KC latency delay. A. The distance between anterior to posterior channel pairs was plotted as a function of the average KC latency difference between the two channels, for all contact pairs (black circles and red triangles). The linear mixed model regression between anterior to posterior distance and delay for all pairs is plotted as a purple line ($p=0.007$), and after excluding the temporal pairs (plotted with red triangles), is plotted as a green line ($p=0.08$). B. The distance between the same anterior to posterior channel pairs as in A was plotted as a function of each individual KC latency difference (black circles and red triangles). A linear mixed model regression calculated to determine if a significant relationship existed for individual KCs on these pairs was significant at $p<10^{-4}$ (purple line). Excluding the temporal pairs plotted with red triangles, the linear mixed model regression was still significant at $p=0.003$ (green line).

Figure 12. Comparison of stage 2 (N2) and stage 3 (N3) KCs. A. Waveforms of averaged N2 and N3 KCs overlaid for subject 1's four channels exhibit highly similar KC morphology. B. Multichannel KC participation is not consistently greater in N2 or N3. The percentage of KCs occurring in each number of channels for N2 (red) and N3 (blue) are plotted for subjects 4, 6 and 9. Subjects 6 and 9 show N2 KCs involving more channels, but this is not the pattern seen in all subjects, as shown with subject 4. When a Chi-squared test was performed for each subject on these distributions, only subjects 6 ($p=0.011$) and 9 ($p=0.000056$) exhibited significant differences.

Figure 13. Summary of current KC findings compared to previous views. A. Previous scalp EEG and intracranial studies of the KC and isolated SOs (i.e. KCs) find the largest amplitude KCs in midline prefrontal regions (orange star), as well as strong (blue arrow), one-directional (faded orange background) propagation from anterior to posterior cortical regions. B. Our

eNeuro Accepted Manuscript

current findings indicate that when measured locally, KCs are actually smallest in amplitude in anterior prefrontal regions (orange star). KCs may co-occur (uniform yellow background) across variably small or large areas of cortex (stars and arrows). Propagation may occur from anterior to temporal regions (grey arrow), but also occurs in a variety of patterns across the cortex (groups of colored arrows). This variability in KC onset, extent, and spread could be used by the cortex during replay to consolidate memories encoded with correspondingly variable spatiotemporal encoding patterns.

Tables

Table 1. Patient information

Subject	Gender	Age	Handedness	Clinical Diagnosis	Pathological Diagnosis	Imaging	Focus	IQ (FSIQ)
Sub1	M	45	L	CPS; Bitemporal	No pathology obtained		Left and right mesial temporal lobes	83
Sub2	F	58	R	CPS; possible generalized epilepsy	No pathology obtained		Likely generalized	80
Sub3	F	45	R	CPS; Multifocal	Multifocal: temporal, parietal, occipital		Temporal	Average
Sub4	F	65	R	CPS; Temporal lobe	No pathology obtained		Right subfrontal & anterior	101

eNeuro Accepted Manuscript

				epilepsy with two foci: left mesial temporal structures & right subfrontal region			temporal	
Sub5	F	27	R	Right temporal lobe epilepsy	No pathology obtained	Right hippocampal sclerosis	Hippocampus, entorhinal cortex, amygdala	Average
Sub6	F	32	R	Left temporal lobe epilepsy	Non-specific gliosis	Normal	Hippocampus, entorhinal cortex, amygdala	77
Sub7	F	23	R	Right temporal lobe epilepsy	Type I focal dysplasia	Normal	Hippocampus, entorhinal cortex, anterior insula	86
Sub8	F	28	R	Right temporal occipital epilepsy	Type II focal dysplasia	Focal cortical dysplasia in right fusiform	Fusiform gyrus, entorhinal cortex	Average
Sub9	F	50	R	Right temporal occipital epilepsy	No pathology obtained	Normal	Right fusiform gyrus	110

1331

eNeuro Accepted Manuscript

1332 Table 2. Mean and standard deviation of maximum KC peak differences

Subject	Number of channels	Mean of maximum KC peak differences (ms)	Standard deviation (ms)
Sub1	4	61.1	49.5
Sub2	13	99	59.6
Sub3	5	86.3	59.5
Sub4	7	66.3	54.1
Sub5 N1	5	24.8	23.8
Sub5 N2	5	27.8	26.4
Sub5 N3	5	32.2	27.7
Sub6 N1	7	71.3	48.5
Sub6 N2	7	66.4	45.6
Sub6 N3	7	81.2	52.8
Sub6 N4	7	60.3	54
Sub7 N1	8	68.6	59.1
Sub7 N2	8	63.2	57.2
Sub7 N3	8	73.4	61.2
Sub7 N4	8	77.7	63.1
Sub7 N5	8	70.7	51.1
Sub7 N6	8	74.9	59.7
Sub8 N1	4	49.8	53.4
Sub8 N2	4	79.2	42

eNeuro Accepted Manuscript

Sub8 N3	4	67.5	59.7
Sub9 N1	2	95.2	59.4
Sub9 N2	2	115.2	0
Sub9 N3	2	52.2	39
Sub9 N4	2	78.6	83

1333

1334 Table 3. Fisher's exact test for co-occurrence.

Subject	1 Channel & 2+ Channels	1 Channel & 3+ Channels	1 Channel & 4+ Channels	1 Channel & 5+ Channels
Sub1	**< 2.2E-16**	**9.49E-12**	**0.000445**	
Sub2	**< 2.2E-16**	**< 2.2E-16**	**< 2.2E-16**	**< 2.2E-16**
Sub3	**< 2.2E-16**	**< 2.2E-16**	**6.24E-09**	0.00493
Sub4	**< 2.2E-16**	**< 2.2E-16**	**5.38E-08**	
Sub5 N1	**< 2.2E-16**			
Sub5 N2	**5.40E-14**			
Sub5 N3	**2.96E-13**	0.0135		
Sub6 N1	**< 2.2E-16**	**< 2.2E-16**	**< 2.2E-16**	**1.10E-15**
Sub6 N2	**< 2.2E-16**	**< 2.2E-16**	**< 2.2E-16**	**< 2.2E-16**
Sub6 N3	**< 2.2E-16**	**< 2.2E-16**	**< 2.2E-16**	**1.25E-15**
Sub6 N4	**3.92E-10**	0.0125		
Sub7 N1	**< 2.2E-16**	**2.33E-06**		
Sub7 N2	**< 2.2E-16**	**1.20E-05**		
Sub7 N3	**< 2.2E-16**	**1.61E-05**	0.0140	

eNeuro Accepted Manuscript

Sub7 N4	**< 2.2E-16**	**2.00E-08**		
Sub7 N5	**9.50E-06**			
Sub7 N6	**8.09E-08**			
Sub8 N1	**< 2.2E-16**	**0.000355**		
Sub8 N2	0.00227			
Sub8 N3	**0.000107**			
Sub9 N1	0.215			
Sub9 N2	0.497			
Sub9 N3	**0.000312**			
Sub9 N4	0.0140			

1335

1336

1337

eNeuro Accepted Manuscript

A

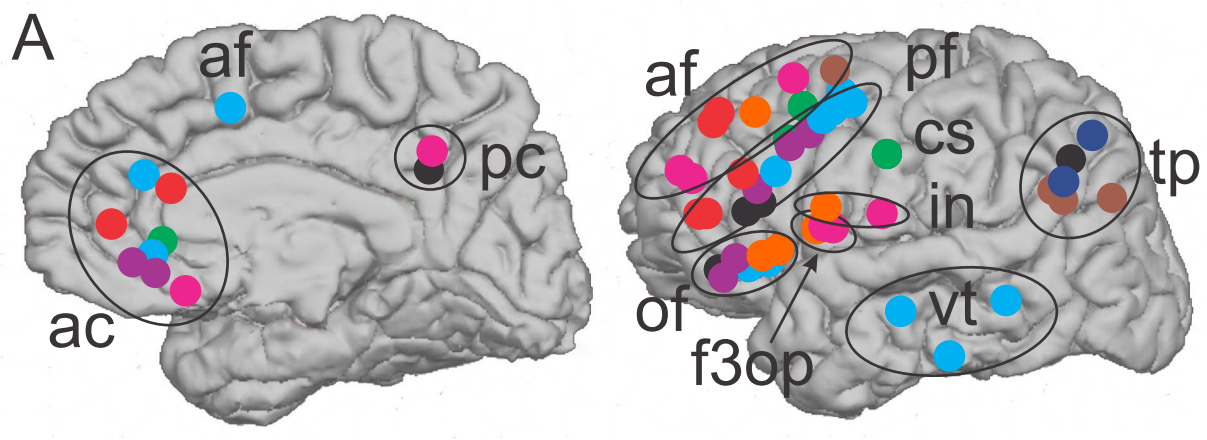

ac-anterior cingulate and subcallosal
af-anterior prefrontal cortex
pc-posterior cingulate
pf-posterior prefrontal cortex
cs-central sulcus
in-insula
f3op-inferior frontal gyrus; pars opercularis
of-orbitofrontal cortex
tp-temporo-parieto-occipital junction
vt-ventrolateral temporal cortex

- Subject #1
- Subject #2
- Subject #3
- Subject #4
- Subject #5
- Subject #6
- Subject #7
- Subject #8
- Subject #9

B

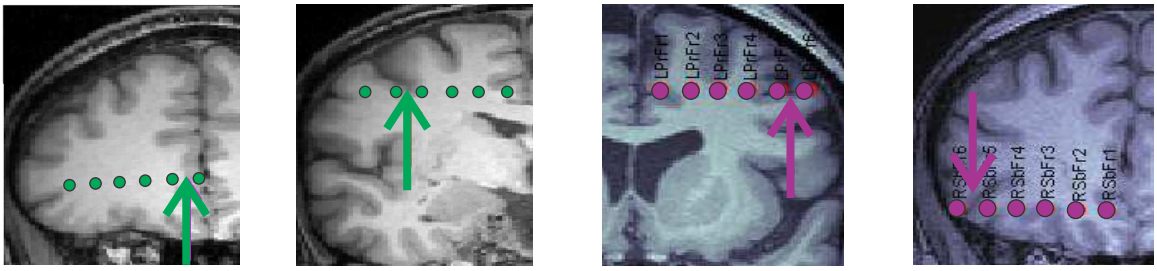

eNeuro Accepted Manuscript

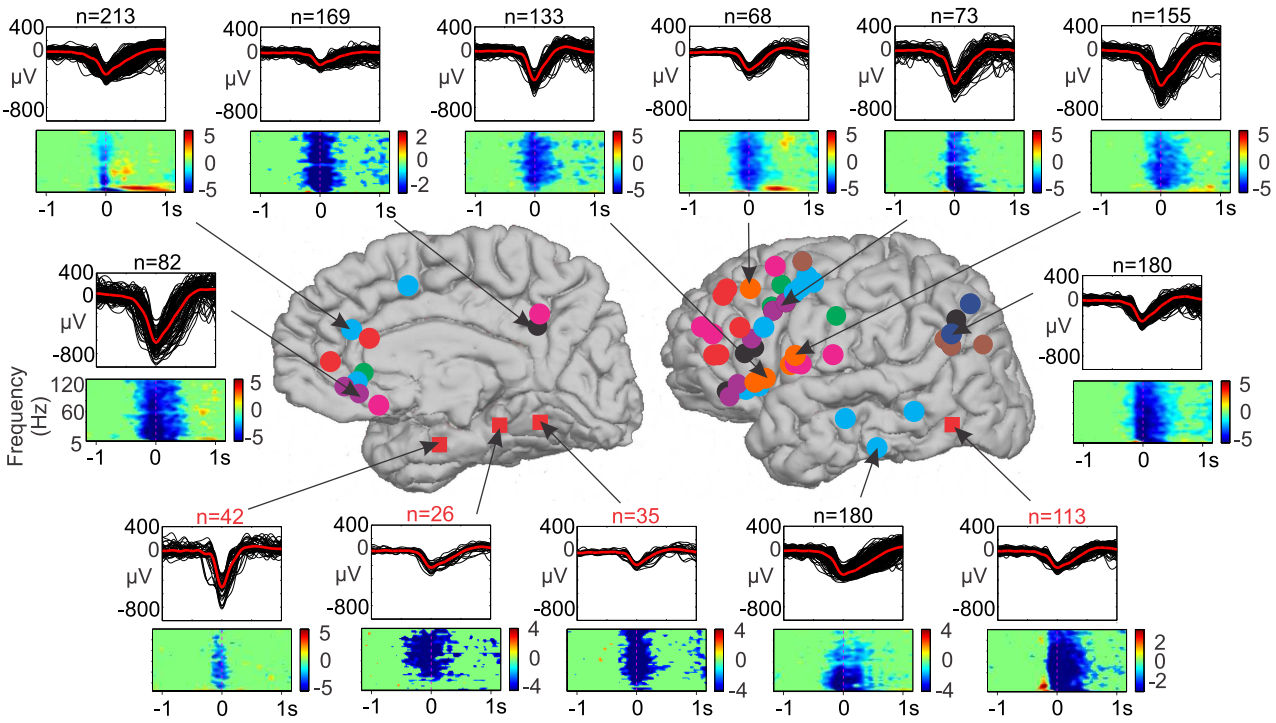

eNeuro Accepted Manuscript

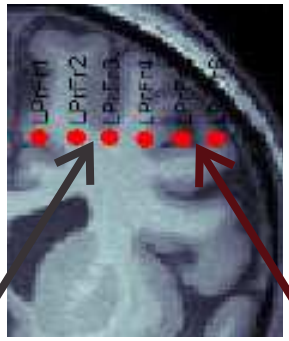

A.
LPF2-3
LPF2 in white matter
LPF3 in white matter
Not included in analysis

B.
LPF5-6
LPF 5 in grey matter
LPF6 in white matter
Included in analysis

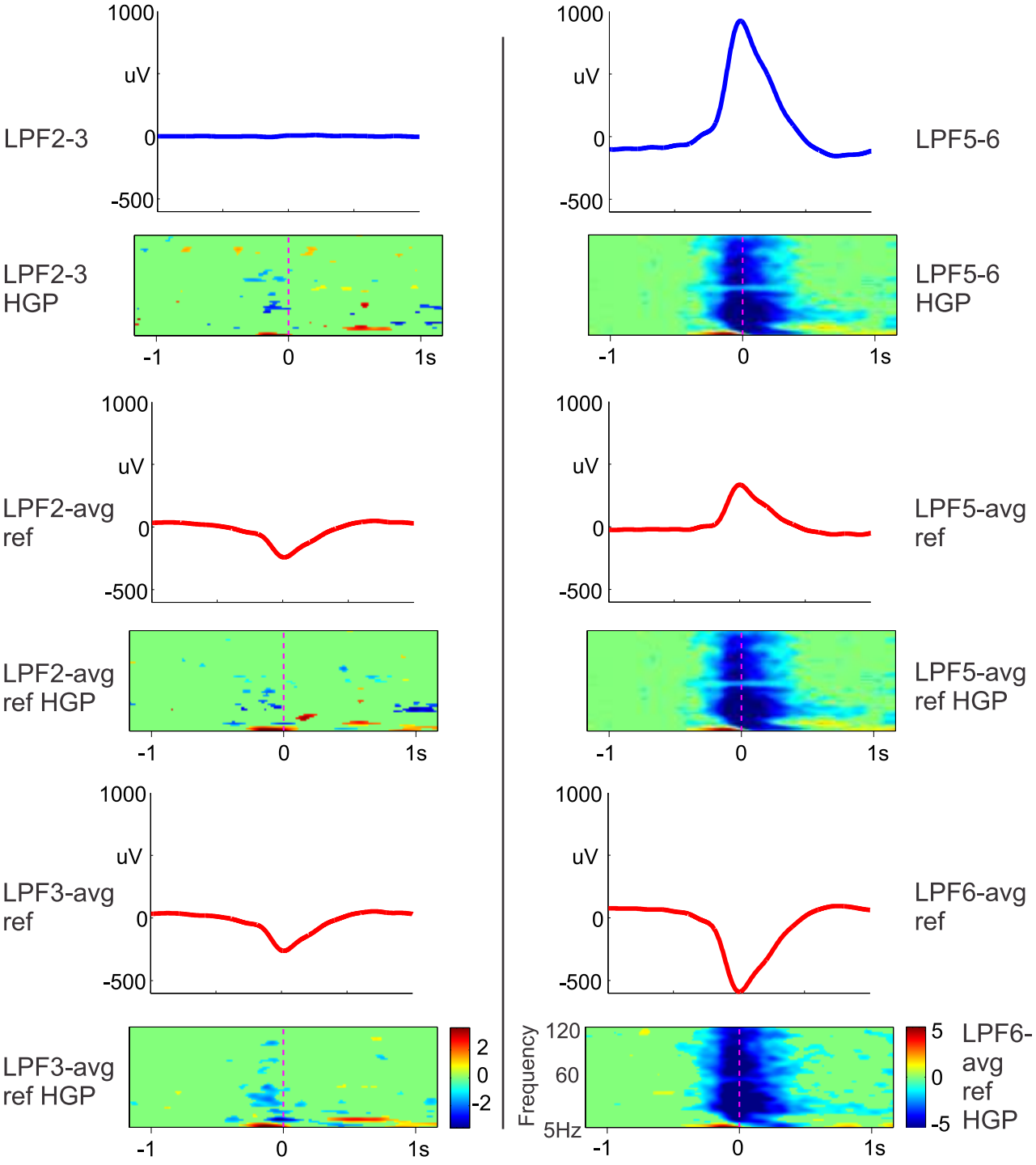

eNeuro Accepted Manuscript

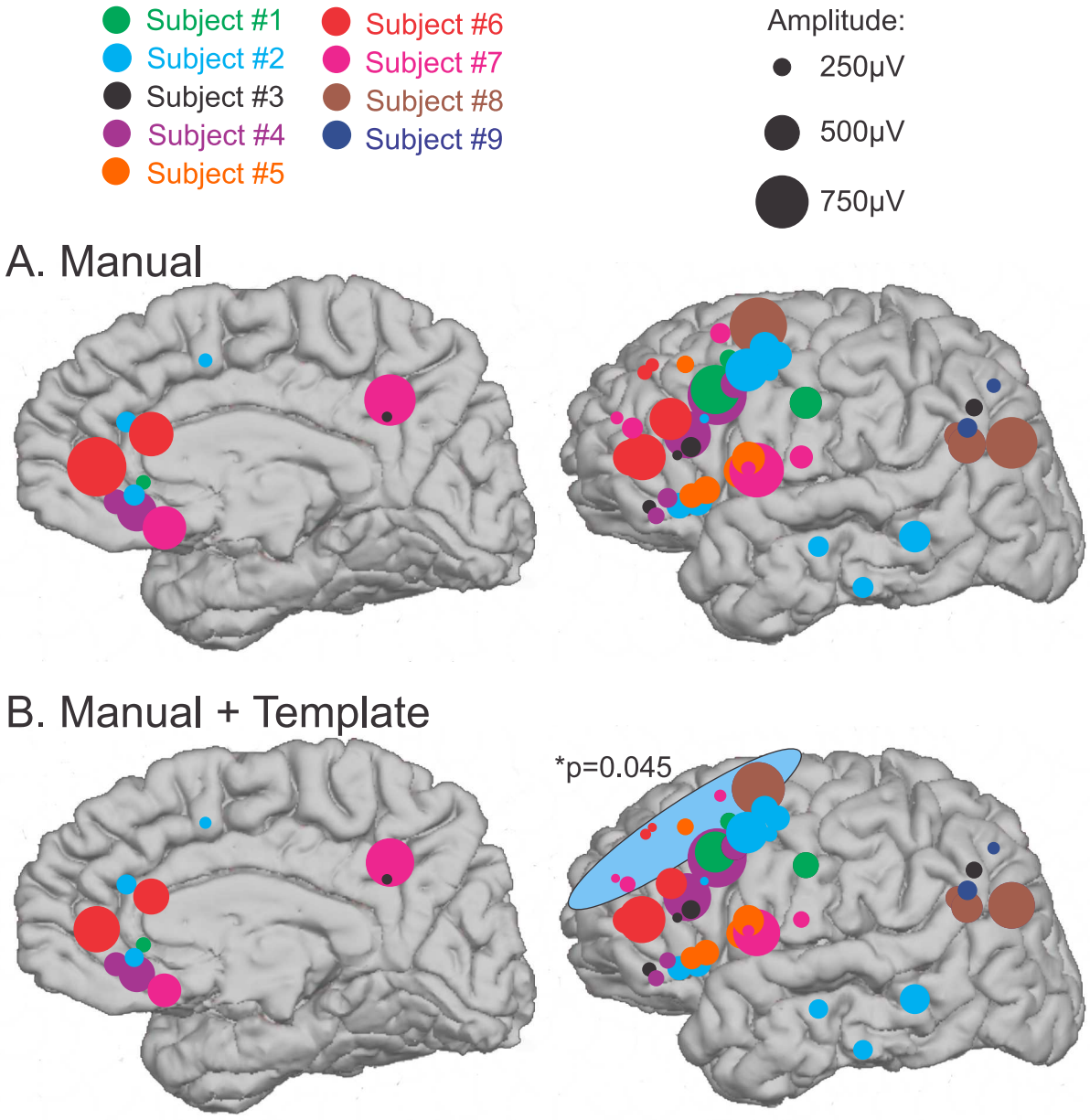

eNeuro Accepted Manuscript

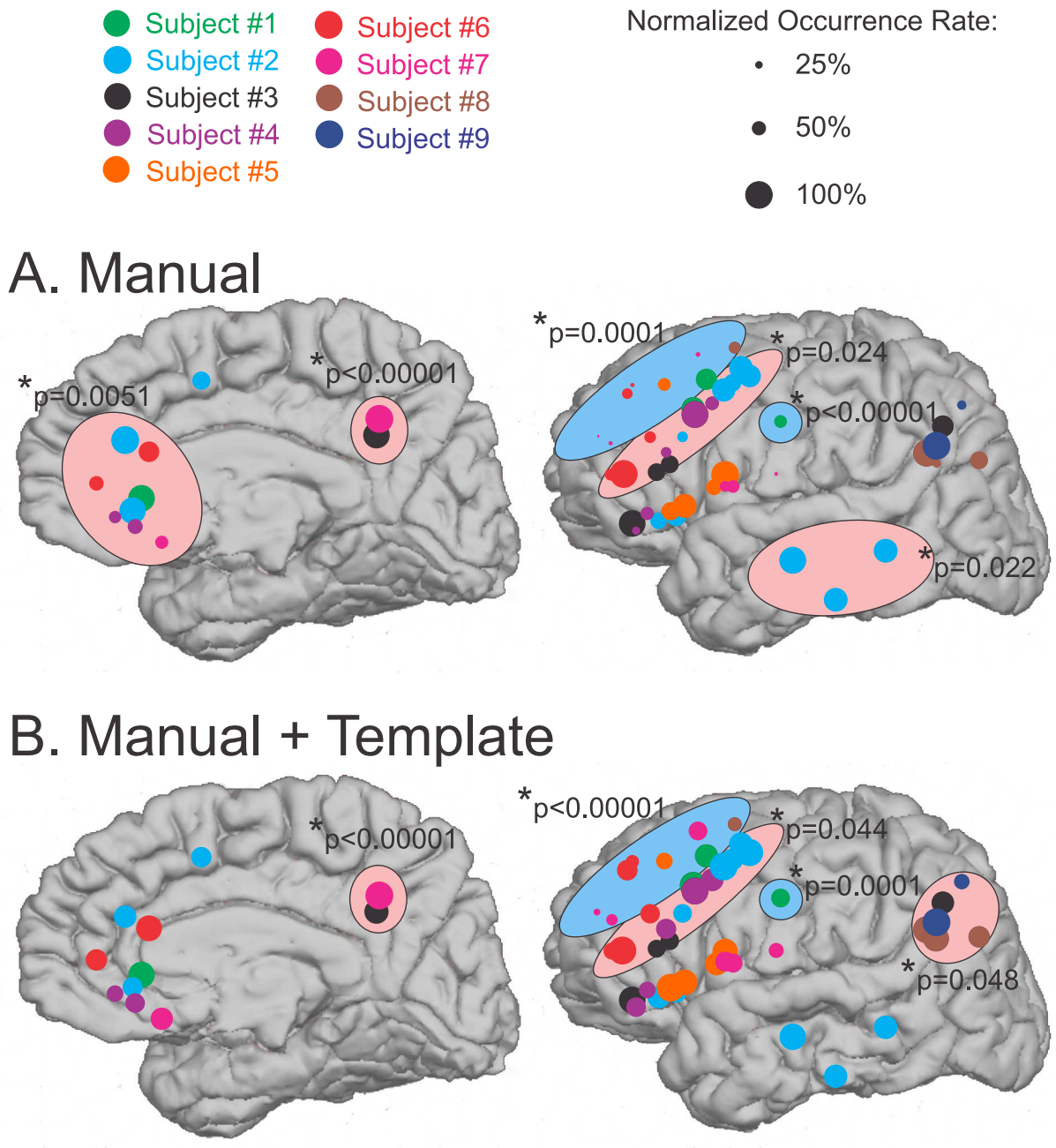

eNeuro Accepted Manuscript

A

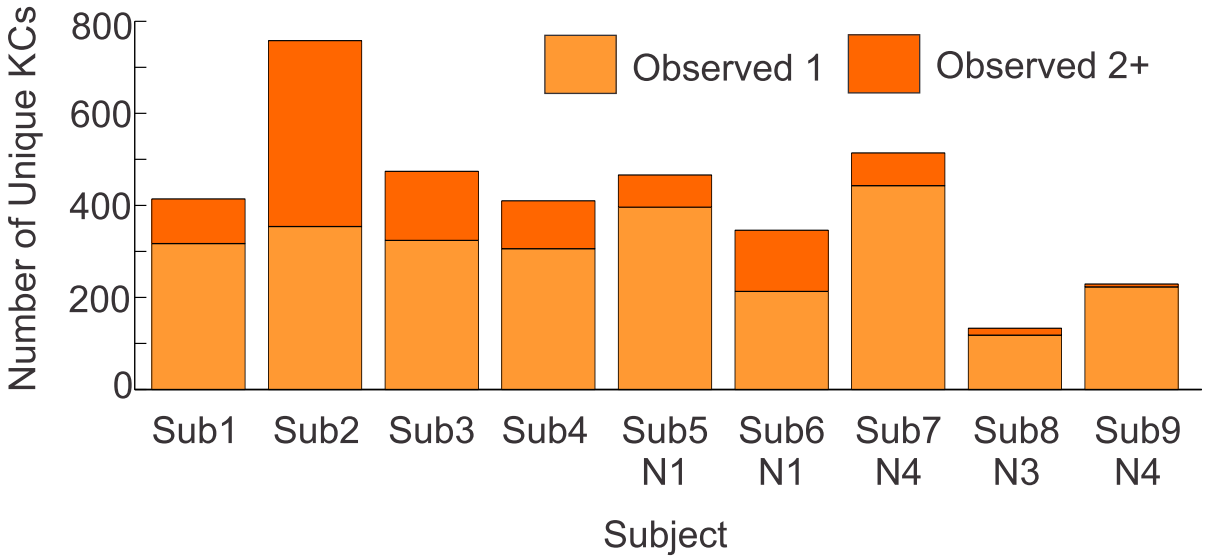

B

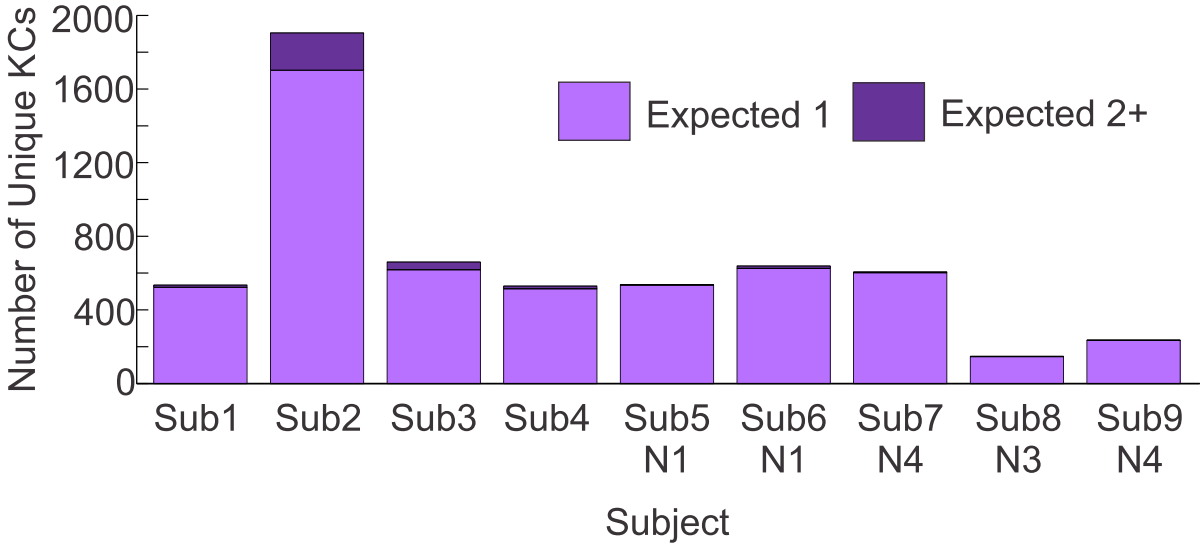

eNeuro Accepted Manuscript

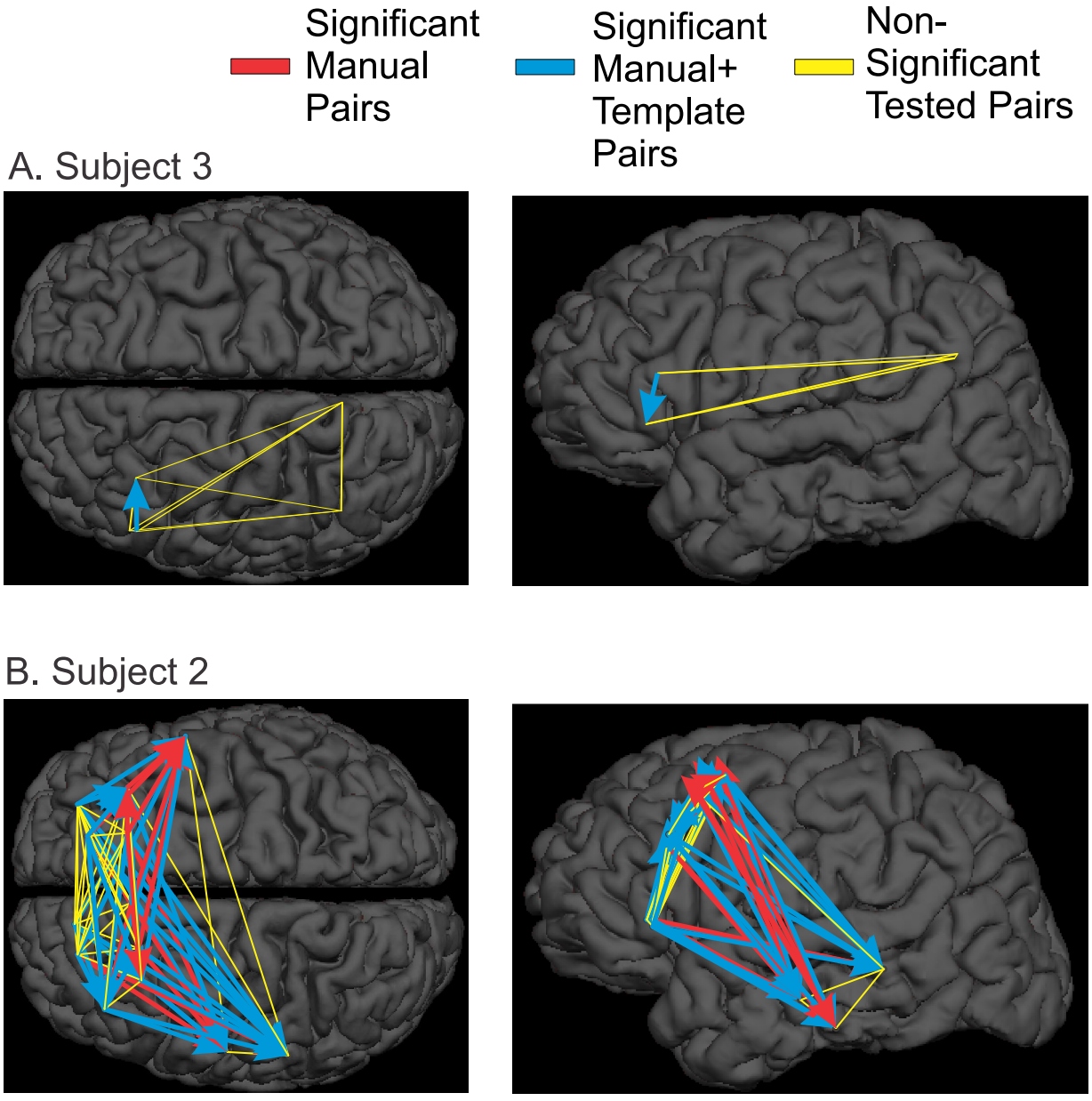

eNeuro Accepted Manuscript

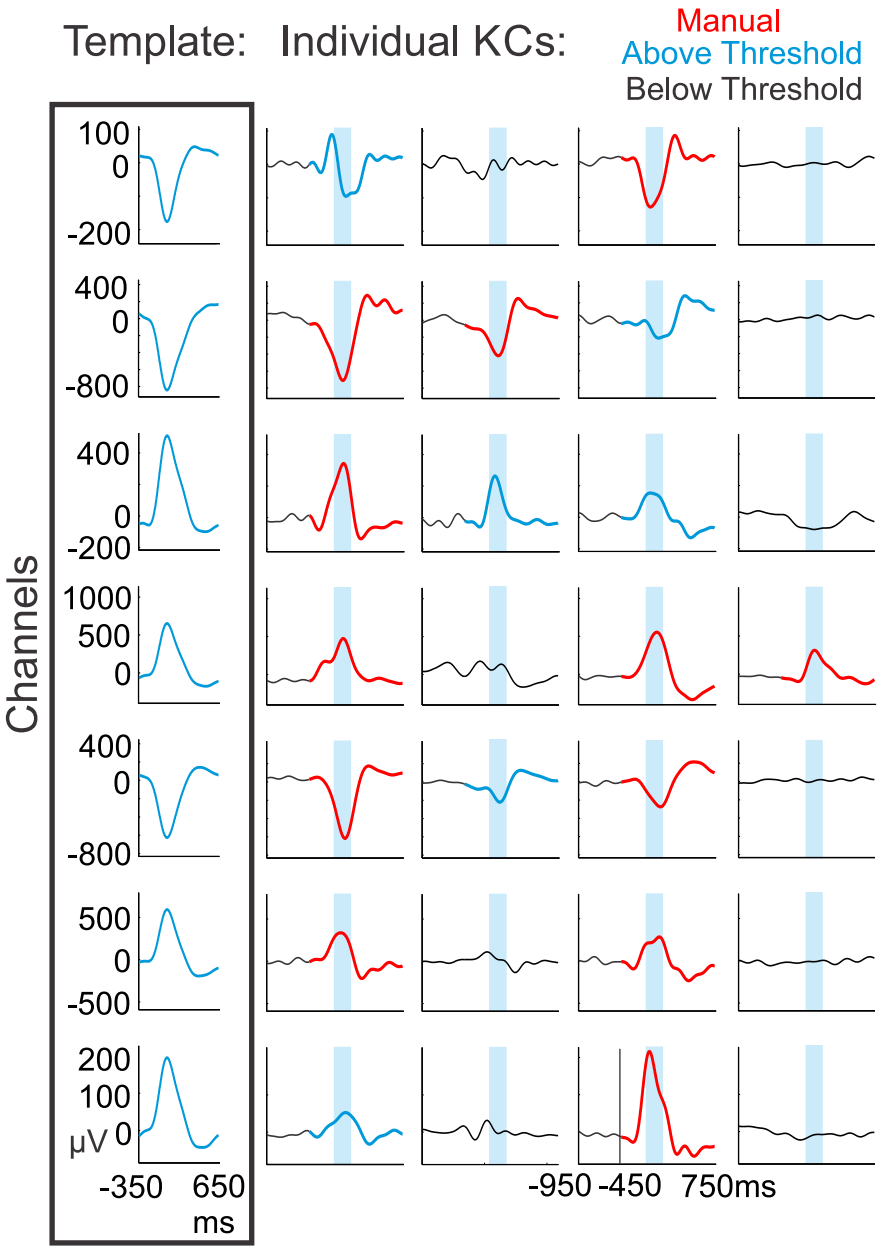

eNeuro Accepted Manuscript

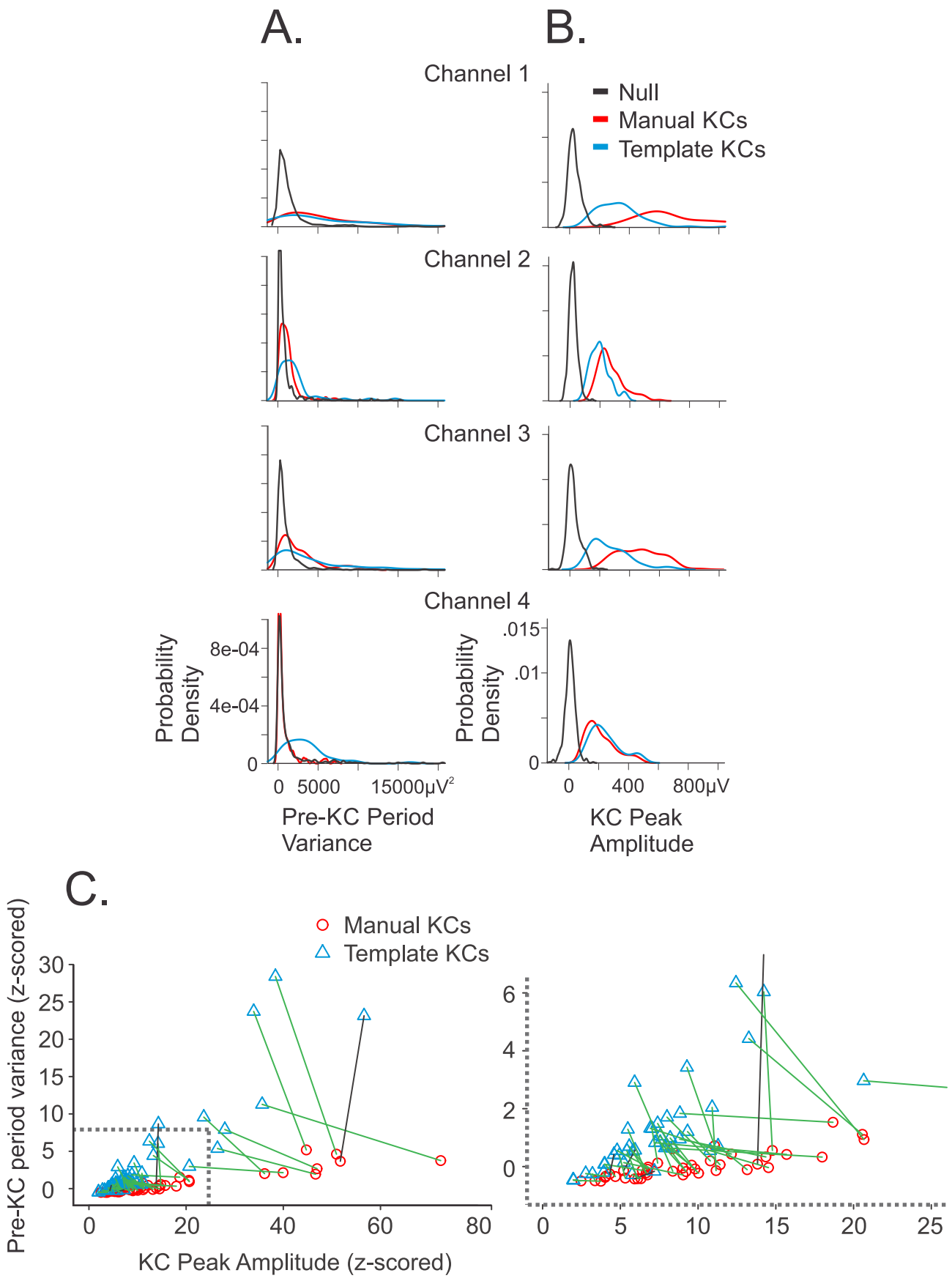

eNeuro Accepted Manuscript

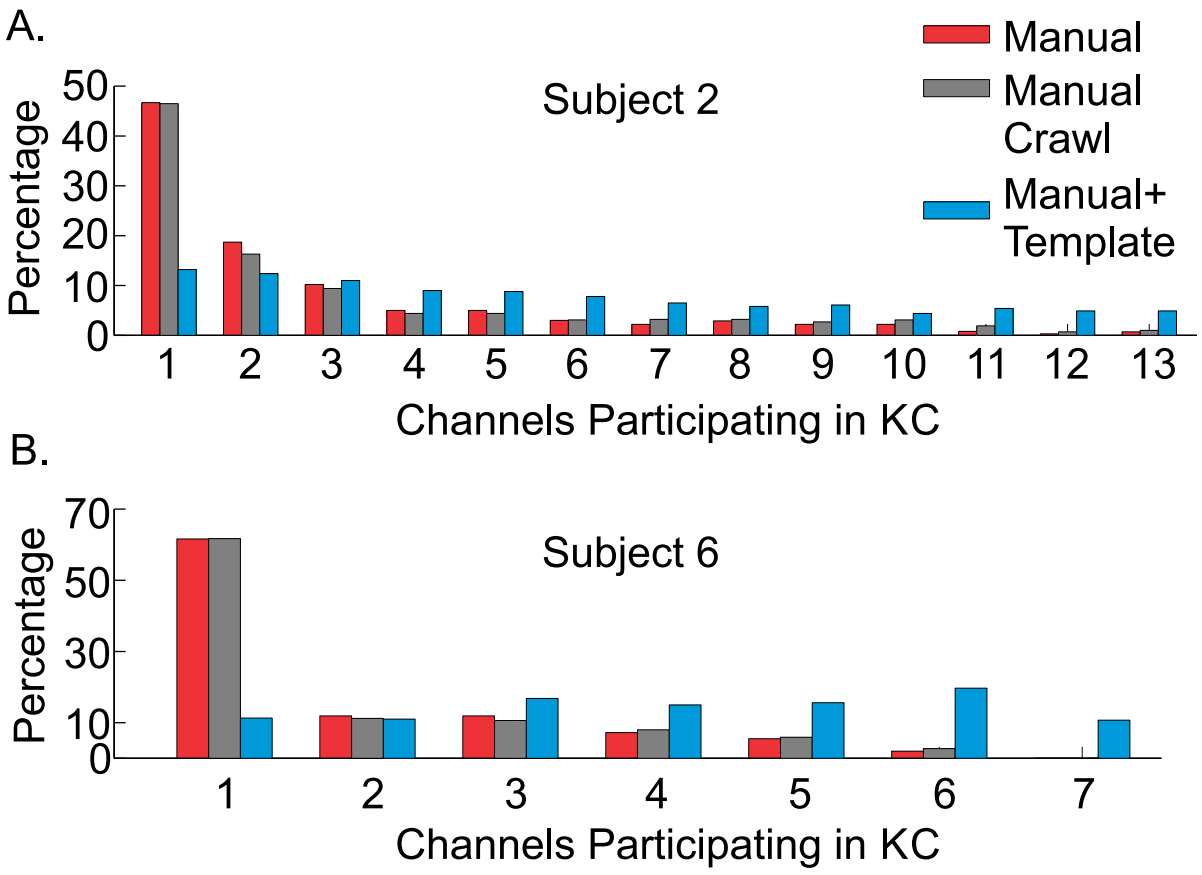

eNeuro Accepted Manuscript

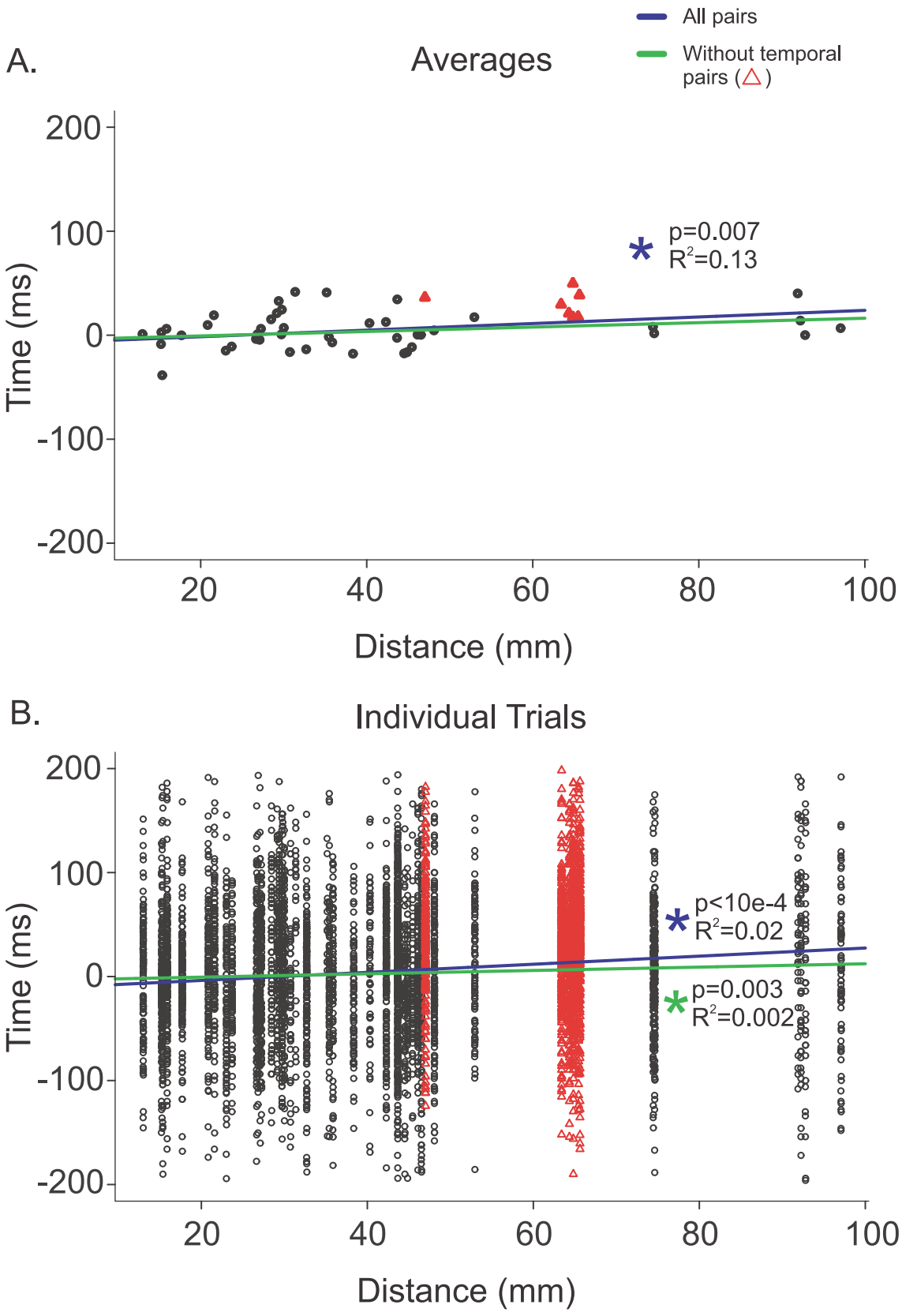

eNeuro Accepted Manuscript

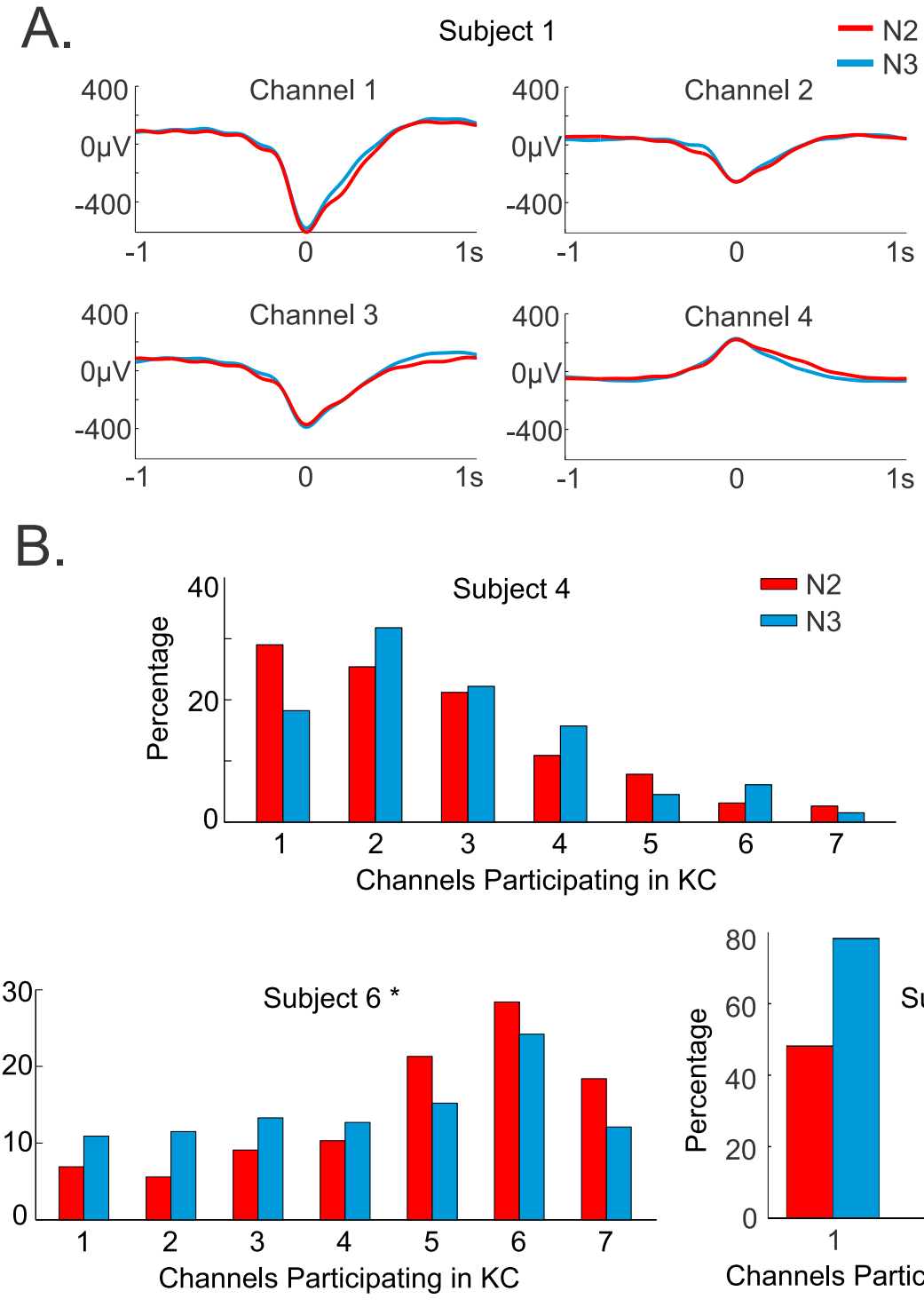

eNeuro Accepted Manuscript